

Evaluation of a Paratuberculosis Quantitative Polymerase Chain Reaction Assay with  
Microscopic Correlation

Ronald Dale Tyler Jr.

Thesis submitted to the faculty of the Virginia Polytechnic Institute and State University in  
partial fulfillment of the requirements for the degree of

Master of Science  
In  
Biomedical and Veterinary Sciences

Nammalwar M. Sriranganathan  
Tanya LeRoith  
Gary R. Pickrell  
Mary R. Prater  
Daniel P. Sponenberg

May 1, 2012  
Blacksburg, Virginia

Keywords: Johne's disease, paratuberculosis, histopathology, qPCR

## Evaluation of a Paratuberculosis Quantitative Polymerase Chain Reaction assay with Microscopic Correlation

### ABSTRACT

Paratuberculosis is an intestinal condition in ruminants infected with *Mycobacterium avium* subspecies *paratuberculosis* (MAP) and precedes Johne's disease, a chronic enteric disorder in ruminants caused by MAP infection. Necropsy with histopathology provides definitive diagnosis of Johne's disease and positive culture of MAP from tissues provides definitive diagnosis of paratuberculosis. To determine assay sensitivity, 85 formalin-fixed paraffin-embedded (FFPE) tissues from ruminants diagnosed with Johne's disease were tested with a commercial paratuberculosis quantitative polymerase chain reaction (qPCR) assay and had a sensitivity of 92%. To determine assay specificity, 21 FFPE tissues from animals without gastrointestinal disease combined with 13 FFPE tissues from non-ruminant animals (frog, dove, turtle, dog, and 2 cats) with non-paratuberculosis mycobacterial diseases were tested with the commercial qPCR assay and had a specificity of 100%.

Slides prepared from the FFPE tissue blocks were stained with hematoxylin & eosin (H&E) and Ziehl-Neelsen's (acid fast stain), then examined for granulomatous inflammation and scored on a scale from 0-4 based on the quantity of acid fast bacteria (AFB). Digital microscopy and morphometric software were used to compute an acid fast bacteria area index (AFBAI) to evaluate a more precise correlation with the qPCR results. The quantity of AFB in tissue slides showed medium to strong correlation with the appropriate qPCR results.

The results indicate that the commercial qPCR assay can be used on FFPE tissues with good results and the qPCR results have medium-strong correlation with quantitative acid fast histopathology.

## **Acknowledgements**

There are numerous people that I need to thank for their help in completing this project. I would like to thank my committee members: Drs. Nammalwar Sriranganathan, Tanya LeRoith, Gary Pickrell, Renee Prater and Phil Sponenberg. I really appreciate the time and effort that everyone has given me in guidance, advice and mentorship. I extend my appreciation to the collaborators of this project - the entire team at the John's Disease Testing Center, at the University of Wisconsin, particularly Drs. Michael Collins, Becky Manning, Marie Pinkerton, Ms. Kelly Anklam and Ms. Brenna Kunkel. Your vision and creativity formed the backbone of this project.

This research project would not have been possible without the case material and I am extremely grateful to Drs. Mark Anderson of the University of California-Davis, Curtis Andrew of Oklahoma State University, Tim Baszler of Washington State University, Sean McDonough of Cornell University, Daniel Paulsen of Louisiana State University, and Geoff Saunders of Virginia-Maryland Regional College of Veterinary Medicine for contributing case material (tissue samples) for this study. Additionally I am thankful to Ms. Tracy Fecteau of Tetracore Inc. and Ms. Patricia Kucinski of AES Chemunex Inc. for their technical assistance throughout this research. I'd also like to thank Bill Carswell and Jon Whitney of the Department of Biomechanical Engineering, Virginia Tech, for their computer expertise and help in operating and executing the slide scans to compute the acid fast bacteria indices.

I wish to thank histopathology technicians: Sandra Cheatsy of the University of Wisconsin as well as Jill Songer, Jennifer Rudd and Barbara Wheeler of Virginia-Maryland Regional College of Veterinary Medicine. Thank you for cutting slides, making scrolls for me, and thank you for teaching me how to cut slides, stain slides and make scrolls.

I continue my appreciation to my resident mates: Drs. Natalie Durrett, Anya Hawthorne, Bonnie Brenseke, Ellen Binder, Sarah Hammond, Pablo Piñeyro and Miranda Vieson. Thank you for being there for me a number of times when I came to you with questions. I appreciate and value your friendship and your unwavering moral support. I further extend my thanks to my veterinary pathology mentors: Drs. David Caudell, Bernard Jortner, Tanya LeRoith, Renee Prater, John Robertson, Geoff Saunders, Phil Sponenberg, Nicole Weinstein, and Kurt Zimmerman. Thank you for your guidance, friendship and mentorship. I am thankful for all of my fellow graduate students, my lab mates in the CMMID microbiology. I extend thanks to my fellow paratuberculosis co-researcher, Ms. Gade Kimswatde for all her assistance and thoughts throughout my studies of paratuberculosis. Thank you Ms. Kay Carlson, for ordering the qPCR assays for me as well as your friendship, guidance and technical support throughout this research project.

Penultimate, I extend my thanks to my advisor (Dr. Sriranganathan) for giving me to the opportunity to explore and experience the world of veterinary research in his microbiology laboratory.

Finally, I extend my deepest and most heartfelt appreciation to my family: my wife Carla, daughter Irene, father and mother in law Carlos & Patricia Gutierrez and my parents Ron & Reba Tyler. You compose the epicenter of my life and you have molded me to the person that I am today. Thank you for your encouragement and guidance in everything I do in my life.

**Table of Contents**

Abstract..... ii

Acknowledgements..... iii

Table of Contents..... v

List of Tables and Figures..... viii

List of Abbreviations..... x

Introduction/Justification..... 1

Chapter 1: Literature Review: Pathogenic Mycobacteria & *Mycobacterium avium*  
subspecies *paratuberculosis*..... 2

    Mycobacteria..... 2

    Tuberculosis Mycobacteria..... 3

    Leprosy Mycobacterium..... 4

    Non-tuberculosis Mycobacteria (NtM) / Atypical Mycobacteria (AtM) /  
Mycobacteria other than tuberculosis (MOTT)..... 5

    Paratuberculosis..... 6

        Johne’s disease clinical signs..... 6

        Johne’s disease lesions..... 6

        Johne’s disease pathogenesis & immunology..... 7

        Paratuberculosis epidemiology, prevalence, & economic impact..... 9

        Crohn’s disease & other human disease potentially associated with  
MAP infection..... 9

            Reports for the association of MAP with Crohn’s disease..... 10

            Reports & arguments against the association of MAP with Crohn’s

disease.....	11
Other human disease potentially associated with MAP.....	12
Paratuberculosis diagnostic assays.....	12
Paratuberculosis control.....	15
References.....	17
Chapter 2: Evaluation of a Commercial Paratuberculosis Real-Time Quantitative Polymerase Chain Reaction Assay on Formalin-Fixed Paraffin-Embedded Tissues for the Detection of <i>Mycobacterium avium</i> subspecies <i>paratuberculosis</i> .....	
	35
Abstract.....	35
Introduction.....	37
Materials and Methods.....	39
Johne’s disease histopathology.....	39
FFPE Scroll Sampling and DNA extraction.....	40
MAP qPCR.....	40
Results.....	41
Discussion & Conclusions.....	42
Sources and manufacturers.....	44
References.....	51
Chapter 3: Correlation of a Quantitative Histopathology with Quantitative Polymerase Chain Reaction in the Diagnosis of Johne’s disease.....	
	54
Abstract.....	54
Introduction.....	56
Materials and Methods.....	60

Acid Fast Score (AFS).....	60
Acid Fast Bacteria Area Index (AFBAI).....	61
MAP Quantitative PCR (qPCR) testing.....	63
Results.....	64
Discussion & Conclusions.....	66
Sources and manufacturers.....	67
References.....	77
Conclusions.....	83
Summary.....	83
Conclusions.....	83

## List of Figures and Tables

	Page
Chapter 2 Figures	
<b>Figure 2.1:</b> Correlation between BioRad iCycler and Stratagene Mx3005p light detecting thermocycler MAP <i>hspX</i> qPCR results	46
Chapter 2 Tables	
<b>Table 2.1:</b> Negative cases	47
<b>Table 2.2:</b> Fecal MAP culture positive Johne's disease cases	48
<b>Table 2.3:</b> Additional Johne's disease cases	49
<b>Table 2.1:</b> Comparison of MAP <i>hspX</i> qPCR with different assays	50
Chapter 3 Figures	
<b>Figure 3.1:</b> Example acid fast scores: Representative acid fast score (AFS) of 1, one macrophage with intracellular acid fast bacteria (AFB) ( <b>arrow</b> ) ( <b>A</b> ), AFS of 2 showing scattered macrophages with scattered macrophages containing intracellular AFB ( <b>B</b> ) AFS of 3 showing moderate numbers of macrophages containing intracellular AFB ( <b>C</b> ) AFS of 4 showing numerous macrophages with intracellular AFB ( <b>D</b> ). All tissues are small intestine stained Ziehl-Neelsen's, 400x magnification	69
<b>Figure 3.2:</b> Example of 5x objective scans of slides used to calculate the total the total tissue area (TTA): A 7 x 4 grid (28 images) Black & White image ( <b>A</b> ), 7x4 grid image with florescent camera ( <b>B</b> ), overlay of black and white and florescent image ( <b>C</b> ), Identification of total tissue area in pixels identified as blue ( <b>D</b> ). TTA = sum of all pixels, 1 pixel = 81 $\mu\text{m}^2$ .	70
<b>Figure 3.3:</b> Examples of a 5 x 5 grid (25 images), 20x objective scan of a slide used to calculate the acid fast bacteria area index (AFBAI) in a section of tissue, Ziehl-Neelsen's stain ( <b>A</b> ), the same 5x5 grid imaged with a fluorescent camera highlighting the acid fast bacteria ( <b>B</b> ), the LabView® morphometric software detection of acid fast bacteria highlighted as green in the same 5x5 grid ( <b>C</b> ).	71
<b>Figure 3.4:</b> Rank Correlations between Acid Fast Score (AFS) and MAP qPCR Cycle threshold (Ct)	72
<b>Figure 3.5:</b> Scatterplot matrices of Acid Fast Bacteria Area Index (AFBAI) & MAP qPCR Cycle threshold (Ct) results	73

**Figure 3.6:** Scatterplot matrices showing differences between correlation strengths by iCycler MAP *hspX* qPCR results and acid fast bacteria area index (AFBAI) results.

74

Chapter 3 Tables

**Table 3.1:** BioRad iCycler MAP *hspX* PCR results by acid-fast score for 85 FFPE scrolls from seventy Johne's disease case, plus thirty-four from eight uninfected animals and 6 non-paratuberculosis mycobacterial infected tissues. FFPE blocks contained either small intestine or mesenteric lymph node (or both) with granulomatous inflammation.

75

**Table 3.2:** Average acid fast score (AFS), average iCycler MAP *hspX* qPCR cycle threshold (Ct) results, and correlation statistics by species

76

## List of Abbreviations

AFBAI	Acid Fast Bacteria Area Index
AFB	Acid Fast Bacteria
AFS	Acid Fast Score
AGID	Agarose Gel Immunodiffusion
CD	Crohn's disease
Ct	Cycle threshold
ELISA	Enzyme Linked Immunosorbent Assay
FFPE	Formalin-Fixed Paraffin-Embedded
JD	Johne's Disease
MAP	<i>Mycobacterium avium</i> subspecies <i>paratuberculosis</i>
PCR	Polymerase Chain Reaction
ParaTB	Paratuberculosis
qPCR	real-time quantitative Polymerase Chain Reaction

## **Introduction/Justification**

Paratuberculosis is infection with *Mycobacterium avium* subspecies *paratuberculosis* (MAP) and can result in Johne's disease in ruminants. This disease has a significant economic impact on meat and milk production. Culture of MAP requires special media and takes 4-20 weeks, therefore typical test & cull management strategies to control paratuberculosis utilize antibody based assays that detect anti-MAP antibodies in later stages of paratuberculosis even though specificity and sensitivity of these tests are not as high as culture. Polymerase chain reaction (PCR) assays have sensitivity and specificities that are similar to culture and real-time quantitative PCR (qPCR) assays have higher sensitivities. Both conventional and real-time quantitative PCR assays can be applied on many types of samples from feces to tissues. Conventional MAP PCR assays have been applied on formalin-fixed paraffin-embedded (FFPE) tissue, but there are no studies evaluating commercial real-time quantitative PCR assays on FFPE tissues. Additionally it has been reported that MAP conventional PCR assay electrophoretic band intensities correlate with quantitative histopathology. We hypothesize that commercial paratuberculosis real-time quantitative PCR assays can be applied to FFPE tissues and that the results will correlate with quantitative histopathology.

## **Literature Review: Pathogenic Mycobacteria & *Mycobacterium avium* subspecies *paratuberculosis***

### **Mycobacteria:**

*Mycobacterium* is a genus of the Actinobacteria class of bacteria with a complete taxonomy of: kingdom - Monera, phylum - Actinobacteria, class - Actinobacteria, subclass - Actinobacteridae, order - Actinomycetales, suborder - Corynebacterineae, family - mycobacteriaceae, and genus - *Mycobacterium*. The word *Mycobacterium* is derived from the combination of the Greek words: *Myces* (fungus) and *bakterion* (small rod).<sup>84</sup> Mycobacteria are aerobic, typically non-motile, and have a thick waxy/fatty cell wall making them characteristically acid-alcohol fast.<sup>64</sup> All mycobacteria have a thick cell wall that is hydrophobic, waxy, and rich in mycolic acids.<sup>13</sup> Mycobacteria cell walls are composed of a mycolic acid layer and peptidoglycan layer that are held together by arabinogalactan polysaccharides.<sup>32</sup> This thick waxy wall contributes to the hardness of this bacterial genus. Closely related bacterial genera are *Nocardia*, *Rhodococcus*, and *Corynebacterium*.<sup>30</sup>

The first *Mycobacterium* ever isolated was the tuberculosis bacillus by Robert Koch in 1882. Koch was subsequently awarded the Nobel Prize in medicine for this discovery in 1905. As a consequence of this, a clinically biased medical classification of Mycobacteria divided pathogenic Mycobacteria into three distinct groups.<sup>84</sup> The first group, referred to as the tuberculosis complex, include *M. tuberculosis*, *M. bovis*, *M. africanum*, and *M. microti* that cause the disease tuberculosis (TB).<sup>84</sup> The second group is composed of mycobacteria that cause Hansen's disease (leprosy) and include *M. leprae* and *M. lepromatosis*.<sup>84</sup> Reflecting the clinical bias from human medicine, the third group is referred to as the non-tuberculosis Mycobacteria

(NTM), Mycobacteria other than tuberculosis (MOTT) or atypical Mycobacteria and include all pathogenic mycobacteria other than those that cause tuberculosis or leprosy.<sup>9,64,84</sup>

### **Tuberculosis Mycobacteria**

Infectious diseases are the leading cause of human deaths in the world, and tuberculosis is the most common cause of death of all infectious diseases.<sup>72</sup> Tuberculosis (TB) has been known since the time of Hippocrates and was called “phthisis,” Greek for “wasting away”.<sup>17</sup> Early pathologists, including Rudolph Virchow, believed that tuberculosis was a form of a neoplasm or abnormal gland.<sup>10,100</sup>

Albert Calmette and Camille Guerin developed an avirulent strain of *M. bovis* through multiple passages of the bacterium grown on potato. This strain would later be referred to as the bacilli Calmette-Guerin (BCG) vaccine.<sup>9,84</sup> The BCG vaccine is one of the most widely used human vaccines in the world for the prevention tuberculosis, though its use is controversial due to variable efficacies.<sup>9</sup>

Tuberculosis is initiated by inhalation of the bacterium into the lungs. Expressed bacterial proteins promote phagocytosis by alveolar macrophages.<sup>84</sup> The persistence of the bacterium within the cytoplasm of macrophages is the key pathologic feature of this disease as well as most all other Mycobacterial diseases. The resulting disease is due to the immune response to the intracellular bacteria and subsequent formation of “tubercles” (infected macrophages surrounded by a wall of T-cell lymphocytes and fibroblasts).<sup>34</sup> In the latent form, infected macrophages are walled off within the lungs and no clinical signs are present.<sup>134</sup> In the active form, the “tubercles” erode into airways and blood vessels and result in clinical signs such as persistent coughing, weight loss, coughing up blood, chest pain, fever and fatigue. Extra-

pulmonary infections in regional lymph nodes and disseminated granulomas in other internal organs (e.g. liver, spleen) may occur and dissemination is related to immune status.<sup>55</sup> Tuberculosis in individuals with immune deficiencies is more prone to dissemination.<sup>5</sup> Additionally, tuberculosis serves as a sentinel disease for HIV infection.<sup>5</sup>

Streptomycin was the first effective treatment of tuberculosis. Subsequently, a multi-mechanistic form of treatment using antibiotic combinations of isoniazid, rifampin, and pyrazinamide given over a period of 6-months, which prevented drug resistance and improved bacterial killing.<sup>112</sup> This treatment was referred to as the short course chemotherapy (SCC) and patients with active or latent tuberculosis have cure rates of >90%.<sup>112</sup>

Diagnosis of tuberculosis is made by a combination of pulmonary radiographs, smears of sputum samples, and/or molecular diagnostics of sputum samples. Exposure to *M. tuberculosis* is indicated by a positive tuberculin-purified protein derivative (PPD) skin test.<sup>3</sup>

### **Leprosy Mycobacteria**

Hansen's disease (leprosy) can be caused by *Mycobacterium leprae* or *M. lepromatosis*. The leprosy bacterium was first described by Norwegian physician A.H. Hansen in 1874.<sup>9</sup> Despite being a well described disease, there are no reports of successful culture of the bacterium.<sup>9</sup> Hansen's disease (HD) is principally a skin disease with a wide variety of lesions. A patient with HD is defined by the World Health Organization (WHO) as having one or more of the following characteristics: 1) hypopigmented or reddish skin lesion(s) with definite loss of sensation, 2) involvement of the peripheral nerves, as demonstrated by definite thickening with loss of sensation, and 3) skin smear with acid-fast bacilli.

The WHO further classifies as HD as paucibacillary or multibacillary based on the number of positive or negative skin smears (<http://www.who.int/lep/classification/en/>). Diagnostic assays for HD include serologic assays, slit-skin smears, biopsies with histopathology, the lepromin test, and PCR assays.<sup>103</sup> Like TB, treatment of HD is based on multi-drug therapy and the WHO recommended treatment regimen includes dapsone, rifampin, and clofazimine and requires a long duration of treatment (years) with several follow-up evaluations to assess treatment success.<sup>81</sup>

### **Non-tuberculosis Mycobacteria (NtM) / Atypical Mycobacteria (AtM) / Mycobacteria other than tuberculosis (MOTT)**

Mycobacteria other than tuberculosis (MOTT), Non-tuberculous Mycobacteria (NtM), and Atypical Mycobacteria (AtM) are considered environmental mycobacteria and cause a broad spectrum of disease in humans and animals. Buruli ulcers caused by *Mycobacterium ulcerans* have become the third most common mycobacterial disease after tuberculosis and leprosy.<sup>14</sup> Approximately 50 different non-tuberculous mycobacterial species have been described that cause diseases in humans.<sup>68</sup> *Mycobacterium marinum* is an atypical mycobacterium that causes a skin disease in humans referred to as swimming pool granulomas.<sup>83</sup> *Mycobacterium avium* complex (MAC) is composed of several subspecies of *Mycobacterium avium* including: *M. avium avium* (MAA), *M. avium intracellulare* (MAI), *M. avium scrofulaceum* (MAS), and *M. avium paratuberculosis* (MAP).<sup>58</sup> While skin diseases are the majority of clinical diseases associated with atypical mycobacterial species, MAC species with the exception of MAP, are typically associated with pulmonary disease.<sup>58</sup> Infection with MAC is an emerging disease, and is particularly important in patients with immune deficiency.<sup>51</sup> However, patients without overt

immune deficiencies have rarely been reported with pulmonary mycobacteriosis caused by MAC.<sup>90</sup>

### **Paratuberculosis**

Paratuberculosis is a condition in ruminants that are infected with *Mycobacterium avium* subspecies *paratuberculosis* (MAP). This condition precedes Johne's disease, a chronic enteric disorder caused by MAP infection. The clinical disease and acid fast bacteria were first reported in 1905 by Drs. Heinrich Johne and Langdon Frothingham.<sup>99</sup>

### **Johne's disease clinical signs**

Clinical signs in ruminants with Johne's disease are associated with gastrointestinal dysfunction. The most common clinical sign in cattle is chronic weight loss with persistent fetid diarrhea, although small ruminants rarely develop diarrhea even in the late stages of the disease.<sup>15</sup> Bottle jaw (submandibular edema) and generalized edema may develop secondary to the chronic protein losing enteropathy. While usually infected in the first months of life, the majority of ruminants do not progress to clinical disease (emaciation, diarrhea in some species) for several years.<sup>135</sup>

### **Johne's disease lesions**

The spectrum of lesions in cases of Johne's disease is based on the stage of infection.<sup>45</sup> A common gross lesion in clinically ill cattle in later stages of Johne's disease is segmental distal small intestine thickening with a corrugated mucosal surface.<sup>15,29,85</sup> Additionally, mineralization of lymphoid tissues and large arteries, associated with chronic infection has been described.<sup>140</sup>

Microscopic intestinal lesions are characterized by focal, multifocal, or segmental mucosal infiltration by macrophages and multinucleate giant cells that may contain few (paucibacillary) to numerous or innumerable (multibacillary) acid-fast bacterial rods and other infiltrating leukocytes (e.g. lymphocytes).<sup>15,29,45,85</sup> The adjacent lymphoid tissue (Peyer's patches) and mesenteric lymph nodes may be infiltrated by similar inflammatory cells.<sup>15,29,85</sup> In earlier stages of infection, gross lesions may be absent and acid-fast organisms may be so few as to be undetectable.<sup>45</sup> In addition to the typical lymphadenitis and enterocolitis, granulomatous inflammatory lesions may extend to the rectum and the liver.<sup>15</sup>

MAP bacteria undergo phagocytosis by macrophages and infected macrophages localize along the intestinal tract, particularly the distal small intestine, cecum, or proximal large intestine, and adjacent mesenteric lymph nodes. Granulomatous inflammation of affected organs is the earliest detectable microscopic lesion.<sup>45</sup> Reported grading systems/scores for Johne's disease report the number of acid-fast bacteria within lesions are variable and correlate with stage of infection.<sup>20</sup>

### **Johne's disease pathogenesis & immunology**

The most common route of infection is through ingestion of MAP contaminated feces, milk or colostrum. The initial contact with the innate immune system is at the epithelial barrier. MAP is transported across the epithelial barrier by specialized microfold epithelial cells that are located among follicle-associated epithelial cells overlying Peyer's patches.<sup>107</sup> Several pattern recognition receptors (PRRs) are involved in the recognition of MAP by epithelial, lymphoid, and histiocytic cells. Several toll like receptors (TLR-1, 2, 4, 5, 6, 8 & 9)<sup>40,74,87,89,124,131</sup> have been reported to play a role in the immune response to MAP. TLR-9 is reported to mediate

internalization of MAP into epithelial microfold cells.<sup>89</sup> After the bacteria are internalized by intestinal epithelial cells they are transported to inter-epithelial leukocytes. Internalization of MAP into inter-epithelial macrophages is also believed to be mediated by toll-like receptors. Interactions with toll-like receptors directly affect the adaptive immune response and these interactions may explain why mutations of TLR 2 & 4 have been associated with increased susceptibility to paratuberculosis in cattle.<sup>96</sup> Additionally, attachment and entry of MAP into macrophages is mediated by the fibronectin receptor and MAP's cell wall fibronectin-attachment protein (FAP)<sup>136</sup> as well as  $\beta$ 2-integrin family (CD11a/CD18), complement receptor (CR3), the mannose receptor and CD14.<sup>113</sup> Once in the macrophage it is believed that MAP survives by inhibiting phagosome and lysosome fusion.<sup>65,141</sup> Inter-follicular regions of the Peyer's patches and mesenteric lymph nodes show the first signs of granulomatous inflammation as early as 2-months after infection. It is believed that MAP is transported to lymph nodes through lymphatics and by circulating monocytes. Activated macrophages and monocytes start producing many important inflammatory cytokines which play a crucial role in the type of adaptive immune response mounted.<sup>119,120</sup>

The adaptive immune response is dynamic as it changes throughout the course of infection (early to late infection) with MAP.<sup>117</sup> The Th<sub>1</sub> immune response is mounted in early MAP infections and during the progression of the disease there is a switch/transition to a Th<sub>2</sub> immune response in late stages of the disease.<sup>117</sup> These assumptions are based on the amounts of IFN $\gamma$  in lesions and the strong correlations with multibacillary or paucibacillary disease.<sup>116</sup>

## **Paratuberculosis epidemiology, prevalence, & economic impact**

International surveillance has confirmed that Johne's disease is a global problem in multiple ruminant species because MAP is distributed worldwide.<sup>125</sup> Individual bovine paratuberculosis prevalence in the US is reported between 5%-18%<sup>44,78</sup> and the herd prevalence is between 50% and 74%.<sup>23,60,133</sup>

Two strains of MAP, referred to as the cow-type or the sheep-type, can be distinguished phenotypically and by genetic analysis, though both of these strains have a broader host range than just cattle and sheep.<sup>22</sup> While MAP is most commonly found infecting domestic and wild ruminants, it has also been detected in non-ruminants.<sup>7,70</sup> Paratuberculosis is of concern for other domestic and free-ranging ruminants such as goats, sheep, deer, and bison.<sup>29,57,85</sup> The reported MAP herd prevalence in small ruminants (sheep & goats) is from 30 to 66%, while the individual prevalence is reported from 2 to 9%.<sup>42,43,138</sup>

The worldwide distribution is representative of the hardiness of the bacteria. MAP bacteria can remain viable in water, feces and cattle slurry for up to 250 days.<sup>66</sup> In the United States the dairy industry loses an estimated 200-250 million dollars annually due to the infection.<sup>61,82</sup> With the economic losses and the increasing prevalence, improving surveillance, prevention and control programs is important. More accurate, fast, and affordable testing methods would greatly aid such programs.

## **Crohn's disease & other human diseases potentially associated with MAP infection**

The possible association between Crohn's disease in humans and paratuberculosis in ruminants is controversial.<sup>53</sup> Crohn's disease is a chronic inflammatory disease in humans that affects the gastrointestinal tract. The disease results in the accumulation of leukocytes in the

lamina propria mucosa leading to villous atrophy. The lesions occur primarily in the terminal ileum and proximal colon and are therefore sometimes referred to as regional or granulomatous enteritis or colitis.<sup>111</sup> Clinical signs associated with the disease include abdominal pain, diarrhea (with visible blood), weight loss, and occasionally vomiting.<sup>48,49</sup> There is no cure for Crohn's disease, and patients have recurring bouts of abdominal pain associated with intestinal inflammation, diarrhea and bleeding throughout their life. Many Crohn's patients and their family members report that stress is an exacerbating factor that promotes the recurrence of clinical signs.<sup>48</sup>

It is generally accepted that both environmental and host genetic factors play a role in Crohn's disease process. Based on geographic and epidemiologic data of the prevalence of Crohn's disease and lactose intolerance, because the incidence of Crohn's disease is lower in populations predisposed to lactose intolerance, it has been hypothesized that an evolutionary relationship between the use of cow milk and human evolution exists.<sup>62</sup>

### **Reports for the association of MAP with Crohn's disease**

Although the exact cause of Crohn's disease is unknown, several publications suggest MAP either plays a role in the pathogenesis or is the putative cause of Crohn's disease.<sup>4,18,19,37,39,41,50,67,73</sup> Even in one of the earliest reported descriptions of Crohn's disease in 1913, Sir. Thomas Dalziel commented that the chronic inflammatory lesion of the intestines of a colleague was similar grossly and microscopically to a recently identified condition in ruminants (Johne's disease) and speculated that the same infectious agent could be responsible.<sup>33</sup>

Gross and microscopic lesions of Johne's and Crohn's diseases are similar. It has also been shown that MAP can be detected in the human milk from lactating women with Crohn's disease.<sup>77</sup> The detection and culture of *MAP* at higher rates from intestines of Crohn's patients

compared to control or patients with ulcerative colitis suggests that *MAP* is associated with Crohn's disease.<sup>16,18,26,56,102,104</sup> One recent study cultured viable *MAP* from buffy coat preparations of peripheral blood in 50% of Crohn's disease patients.<sup>76</sup> This report provides evidence that the bacterium circulates in the peripheral blood of patients with this disease in addition to colonizing the intestinal tract. This report generated much debate and controversy. The author of this report followed it by a blind multi-center investigation, using three independent laboratories to confirm his findings.<sup>75</sup> Further, a report of a focal cluster of Crohn's disease patients in a small urban western city in the United States seemingly suggested a link for *MAP* contamination in the local water source.<sup>86</sup> In addition, the successful treatment of Crohn's patients with antimycobacterials provides further empirical evidence that *MAP* may be involved in the pathogenesis and resulting clinical signs of Crohn's disease.<sup>11,105</sup>

### **Reports & arguments against the association of *MAP* with Crohn's disease**

One report using fluorescent PCR to detect *MAP* failed to detect any genetic material unique to *MAP* in patients with Crohn's disease.<sup>95</sup> Another case-control study based on a 1,030 person questionnaire (218 with Crohn's disease and 812 without Crohn's disease) concluded that consumption of pasteurized milk was associated with reduced risk of Crohn's disease while consumption of meat was associated with an increased risk of Crohn's disease.<sup>1</sup> With the results of this study the researchers concluded that the consumption of dairy products and water, and thus *Mycobacterium avium* subspecies *paratuberculosis* was not associated with Crohn's disease.<sup>1</sup> Another similar questionnaire study from 702 dairy or beef producers (3 with Crohn's disease) and 774 veterinarians (4 with Crohn's disease) also concluded that on the premise of occupational hazards, Johne's disease is not associated with Crohn's disease.<sup>91</sup>

A review of the Crohn's disease pathogenesis summed up several arguments against MAP as the cause of Crohn's disease (CD).<sup>98</sup> It was suggested that culture of MAP from patients with CD could simply be due to a disruption in the mucosal barrier because no acid fast bacteria are visible in lesions of CD patients, and CD patients get better with immunosuppressive drugs whereas typical mycobacterial diseases worsen with immune suppression.<sup>98</sup> Based on this evidence, Crohn's disease may be a result of a complex immune dysfunction, rather than MAP.

### **Other human diseases potentially associated with MAP**

Blau disease in humans is a chronic, familial, granulomatous, multi-centric inflammatory condition (arthritis & uveitis) which has also been postulated to be caused by a combination of MAP infection and NOD2 dysfunction.<sup>36</sup> MAP has also been suggested to play a role in the pathogenesis of Hashimoto's thyroiditis<sup>31,110</sup> and in type 1 diabetes mellitus.<sup>35</sup>

### **Paratuberculosis diagnostic assays**

Accurate and precise identification methods for paratuberculosis and Johne's disease are critical for control of disease as well as MAP surveillance. Both for animal health and economic reasons, efficient, affordable and accurate surveillance tools are necessary for effective MAP infection control.

Definitive diagnosis of Johne's disease is based on gross lesions combined with the typical microscopic lesions (granulomatous enteritis & lymphadenitis often with visible acid-fast bacteria) and detection of MAP in the affected tissues (culture or by polymerase chain reaction (PCR) assays). Tissues at necropsy are fixed in buffered formalin and trimmed and processed into paraffin tissue blocks (formalin-fixed paraffin-embedded (FFPE)). Slides prepared from FFPE tissue sections treated with a variety of stains such as hematoxylin and eosin (H&E) permit

the diagnosis of many diseases. Ziehl-Neelsen's stain is commonly used to identify acid-fast bacteria such as MAP though it is not specific for *Mycobacteria* and also stains other bacteria such as *Corynebacterium* and *Nocardia*.<sup>121</sup> Several immunohistochemical methods have been developed to identify MAP in sections prepared from FFPE tissues, though these techniques are not specific for MAP as other *Mycobacteria* will stain positive.<sup>12,69,121</sup>

Fecal or tissue culture of MAP is traditionally considered the gold standard for the diagnosis of paratuberculosis.<sup>88</sup> However culture can be labor intensive, time consuming, taking up to 4-8 weeks, and can be insensitive if not properly performed.<sup>132</sup> Fecal and environmental samples can be pooled with limited loss of sensitivity to establish the infection status of premises.<sup>130</sup> Culture is generally high for paratuberculosis sensitivity & specificity, however, sub-clinical carriers can intermittently shed MAP in the milk, colostrum and feces and it is postulated that some animals may pass the bacteria transiently without any gross or microscopic lesions.<sup>97,122</sup>

Serologic assays, such as complement fixation (CF), agar gel immunodiffusion (AGID), or enzyme linked immunosorbent assays (ELISAs) provide for a fast turnaround time and are relatively simple to perform, though they are not as accurate as culture and therefore are better suited for herd surveillance.<sup>21,25,106</sup> Multiple commercial ELISA assays have been evaluated and compared to culture and/or PCR assays for the detection of paratuberculosis with similar results.<sup>28,52,118</sup> Two of the more commonly used paratuberculosis ELISAs in the United States are the Parachek® assay by Biocor and the Herdcheck-II® ELISA by Idexx. In these assays serum, plasma or even milk can be used as the test substrate or fluid. The major benefits of the Paratuberculosis ELISAs are low cost and fast turnaround times. Another advantage of paratuberculosis ELISAs is the stability of the test substrate because serum or milk can be

stored for long periods. Though the assays are inexpensive and the turnaround time is quick, the assays can be somewhat labor intensive. The specificity for detecting paratuberculosis with the commercial ELISAs is reported to be high (>95%), however the sensitivity is rather low, between 5-30%.<sup>79,80</sup>

The development of PCR assays for the detection of MAP-specific genetic sequences has greatly expanded the repertoire of diagnostic targets for Johne's disease testing. There are a few common genetic targets used in PCR assays that are specific for MAP. Commonly used MAP specific genetic targets include the insertion sequence 900 (IS900)<sup>92,137</sup>, heat shock proteins X (*hspX*)<sup>38</sup> and F57<sup>129</sup> genes. Conventional PCR assays target and amplify one DNA template, whereas in multiplex PCR assays multiple unique DNA templates are targeted and amplified. Conventional and multiplex PCR assays use gel electrophoresis in the final step of the assays for viewing the DNA product. There is only one copy of the *hspX* and F57 gene in the MAP genome, whereas there are 12-20 copies of the IS900 gene.<sup>59,101</sup> While IS900-like elements have been described in distantly related Mycobacteria,<sup>127</sup> more recent IS900 PCR protocols have been designed to avoid cross-reactions with such IS900-like elements.<sup>54,63</sup>

Commercial real-time, quantitative PCR (qPCR) assays targeting the MAP *hspX* and IS900 genes are now commonly used to detect MAP in fecal samples. While differences have been described between sheep and cow type MAP strains, there are no described differences of IS900 or MAP *hspX* target genes between the sheep and cow type MAP strains. When detecting MAP in feces, these real-time PCR assays are more sensitive and as specific as standard culture methods and much more accurate than serum ELISAs for diagnosing paratuberculosis.<sup>2,128</sup>

The *hspX* commercial real-time qPCR assay has been used to evaluate different methods of extracting DNA from MAP cultures.<sup>126</sup> Direct fecal qPCR is now an accepted diagnostic

assay for the National Voluntary Bovine Johne's Disease Control Program in the United States.<sup>25</sup> The quantitative PCR assays takes less time than traditional PCR, because gel electrophoresis is not required and results are interpreted from the Cycle Threshold (Ct) detected by the real-time PCR thermocycler.

Multiple methods of DNA extraction from FFPE tissues for PCR specific for MAP have been described.<sup>88,139</sup> A simple freeze/boil method for MAP DNA extraction from FFPE tissues has been reported to be consistently effective for detecting MAP specific DNA by IS900 conventional PCR.<sup>139</sup> While this technique was initially applied to conventional IS900 PCR, it can likely be applied to other PCR targets specific for MAP and used for real-time quantitative PCR (qPCR).

With advances in rapid DNA extraction and commercially available paratuberculosis qPCR kits, it is now feasible for any laboratory to obtain Johne's disease diagnostic information via qPCR on FFPE tissues.

### **Paratuberculosis control**

No drugs are approved for the treatment of paratuberculosis, and treatment in ruminant animals is rarely attempted due to the cost, infectious nature, and poor prognosis. Of the few studies of Johne's disease treatment reported and clinical outcome was ultimately unsuccessful though initially clinical signs improved.<sup>71,114,115</sup>

Focus is typically placed on the prevention and control of paratuberculosis rather than treatment. Important management practice addresses the overall cleanliness of the farm, manure handling, newborn-calf care, and restriction of contact between calves and mature animals.<sup>46</sup>

Herd testing & classification is another critical component of the management aspect of controlling Johne's disease. Fecal culture and ELISA serology are the most commonly employed techniques for the detection of MAP.<sup>94</sup> It is currently recommended that combined testing techniques be used in the test and cull management practices. Test and cull programs that use assays with good MAP detection sensitivity are predicted to significantly decrease in MAP prevalence within a herd.<sup>27,47</sup>

Culling positive cows detected by testing of pooled samples by cultures, followed by testing individual cows that are included in positive cultures of pooled samples, or testing individual cows during lactation using serologic assays has been an effective strategy for control. Focusing on a strict test- and- cull protocol and testing cattle during lactation has provided encouraging results from control strategies.<sup>24</sup> However, with the open nature and cross-over of livestock and wildlife ruminants, control measures are not 100% effective.

Preventing paratuberculosis is a challenging endeavor. Vaccines have been developed but are often not used due to interference with tuberculosis surveillance programs. Numerous vaccines have been developed and studied in the control of Johne's disease with most studies reporting vaccination as a valuable tool in reducing microbial contamination risks and control of clinical Johne's disease.<sup>6,108,109</sup> However available vaccines do not fully protect animals from infection, although there is evidence that vaccination does reduce clinical symptoms and decrease fecal shedding of MAP.<sup>93</sup> Commonly used vaccines are either attenuated or killed vaccines.<sup>8</sup> Finally a major drawback in vaccinating for MAP is the interference with diagnostic tests for tuberculosis and subsequently tuberculosis eradication programs.<sup>8,123</sup>

## References:

- 1 Abubakar I, Myhill DJ, Hart AR, Lake IR, Harvey I, Rhodes JM, Robinson R, Lobo AJ, Probert CS, Hunter PR: A case-control study of drinking water and dairy products in Crohn's Disease--further investigation of the possible role of Mycobacterium avium paratuberculosis. *Am J Epidemiol* **165**: 776-783, 2007
- 2 Alinovi CA, Ward MP, Lin TL, Moore GE, Wu CC: Real-time PCR, compared to liquid and solid culture media and ELISA, for the detection of Mycobacterium avium ssp. paratuberculosis. *Vet Microbiol* **136**: 177-179, 2009
- 3 Almeida LM, Barbieri MA, Da Paixao AC, Cuevas LE: Use of purified protein derivative to assess the risk of infection in children in close contact with adults with tuberculosis in a population with high Calmette-Guerin bacillus coverage. *Pediatr Infect Dis J* **20**: 1061-1065, 2001
- 4 Bakker D, Willemsen PT, van Zijderveld FG: Paratuberculosis recognized as a problem at last: a review. *Vet Q* **22**: 200-204, 2000
- 5 Barnes PF, Bloch AB, Davidson PT, Snider DE, Jr.: Tuberculosis in patients with human immunodeficiency virus infection. *N Engl J Med* **324**: 1644-1650, 1991
- 6 Bastida F, Juste RA: Paratuberculosis control: a review with a focus on vaccination. *Journal of Immune Based Therapies and Vaccines* **9**: 8, 2011
- 7 Beard PM, Daniels MJ, Henderson D, Pirie A, Rudge K, Buxton D, Rhind S, Greig A, Hutchings MR, McKendrick I, Stevenson K, Sharp JM: Paratuberculosis infection of nonruminant wildlife in Scotland. *J Clin Microbiol* **39**: 1517-1521, 2001
- 8 Begg D, Griffin J: Vaccination of sheep against M. paratuberculosis: immune parameters and protective efficacy. *Vaccine* **23**: 4999-5008, 2005

- 9 Beutner EH. MR: Mycobacterium. *In: Medical Microbiology*, ed. Milgrom F. FT. Churchill Livingstone, New York, NY, 1982
- 10 Bloom BR: Tuberculosis: Pathogenesis, Protection and Control American Society for Microbiology, Washington D.C., 1994
- 11 Borody TJ, Leis S, Warren EF, Surace R: Treatment of severe Crohn's disease using antimycobacterial triple therapy--approaching a cure? *Dig Liver Dis* **34**: 29-38, 2002
- 12 Brees DJ, Reimer SB, Cheville NF, Florance A, Thoen CO: Immunohistochemical detection of Mycobacterium paratuberculosis in formalin-fixed, paraffin-embedded bovine tissue sections. *J Vet Diagn Invest* **12**: 60-63, 2000
- 13 Brennan PJ, Nikaido H: The envelope of mycobacteria. *Annu Rev Biochem* **64**: 29-63, 1995
- 14 Brown-Elliott BA, Griffith DE, Wallace RJ, Jr.: Newly described or emerging human species of nontuberculous mycobacteria. *Infect Dis Clin North Am* **16**: 187-220, 2002
- 15 Buergelt CD, Hall C, McEntee K, Duncan JR: Pathological evaluation of paratuberculosis in naturally infected cattle. *Vet Pathol* **15**: 196-207, 1978
- 16 Bull TJ, McMinn EJ, Sidi-Boumedine K, Skull A, Durkin D, Neild P, Rhodes G, Pickup R, Hermon-Taylor J: Detection and verification of Mycobacterium avium subsp. paratuberculosis in fresh ileocolonic mucosal biopsy specimens from individuals with and without Crohn's disease. *J Clin Microbiol* **41**: 2915-2923, 2003
- 17 Castiglioni A: History of tuberculosis, vol. 40, pp. 1-96. Medical Life, 1933
- 18 Chiodini RJ, Van Kruiningen HJ, Merkal RS, Thayer WR, Jr., Coutu JA: Characteristics of an unclassified Mycobacterium species isolated from patients with Crohn's disease. *J Clin Microbiol* **20**: 966-971, 1984

- 19 Chiodini RJ, Van Kruiningen HJ, Thayer WR, Coutu JA: Spheroplastic phase of mycobacteria isolated from patients with Crohn's disease. *J Clin Microbiol* **24**: 357-363, 1986
- 20 Clark RG, Griffin JF, Mackintosh CG: Johne's disease caused by *Mycobacterium avium* subsp. *paratuberculosis* infection in red deer (*Cervus elaphus*): an histopathological grading system, and comparison of paucibacillary and multibacillary disease. *N Z Vet J* **58**: 90-97, 2010
- 21 Colgrove GS, Thoen CO, Blackburn BO, Murphy CD: Paratuberculosis in cattle: a comparison of three serologic tests with results of fecal culture. *Vet Microbiol* **19**: 183-187, 1989
- 22 Collins DM, De Zoete M, Cavaignac SM: *Mycobacterium avium* subsp. *paratuberculosis* strains from cattle and sheep can be distinguished by a PCR test based on a novel DNA sequence difference. *J Clin Microbiol* **40**: 4760-4762, 2002
- 23 Collins M, Sockett D, Goodger W, Conrad T, Thomas C, Carr D: Herd prevalence and geographic distribution of, and risk factors for, bovine paratuberculosis in Wisconsin. *Journal of the American Veterinary Medical Association* **204**: 636, 1994
- 24 Collins MT, Eggleston V, Manning EJ: Successful control of Johne's disease in nine dairy herds: results of a six-year field trial. *J Dairy Sci* **93**: 1638-1643, 2010
- 25 Collins MT, Gardner IA, Garry FB, Roussel AJ, Wells SJ: Consensus recommendations on diagnostic testing for the detection of paratuberculosis in cattle in the United States. *J Am Vet Med Assoc* **229**: 1912-1919, 2006
- 26 Collins MT, Lisby G, Moser C, Chicks D, Christensen S, Reichelderfer M, Hoiby N, Harms BA, Thomsen OO, Skibsted U, Binder V: Results of multiple diagnostic tests for

- Mycobacterium avium* subsp. *paratuberculosis* in patients with inflammatory bowel disease and in controls. *J Clin Microbiol* **38**: 4373-4381, 2000
- 27 Collins MT, Morgan IR: Simulation model of paratuberculosis control in a dairy herd. *Preventive Veterinary Medicine* **14**: 21-32, 1992
- 28 Collins MT, Wells SJ, Petrini KR, Collins JE, Schultz RD, Whitlock RH: Evaluation of five antibody detection tests for diagnosis of bovine paratuberculosis. *Clinical and Vaccine Immunology* **12**: 685, 2005
- 29 Corpa JM, Garrido J, Garcia Marin JF, Perez V: Classification of lesions observed in natural cases of paratuberculosis in goats. *J Comp Pathol* **122**: 255-265, 2000
- 30 Cummins CS, Harris H: Studies on the cell-wall composition and taxonomy of *Actinomycetales* and related groups. *J Gen Microbiol* **18**: 173-189, 1958
- 31 D'Amore M, Lisi S, Sisto M, Cucci L, Dow CT: Molecular identification of *Mycobacterium avium* subspecies *paratuberculosis* in an Italian patient with Hashimoto's thyroiditis and Melkersson-Rosenthal syndrome. *J Med Microbiol* **59**: 137-139, 2010
- 32 Daffe M, McNeil M, Brennan PJ: Major structural features of the cell wall arabinogalactans of *Mycobacterium*, *Rhodococcus*, and *Nocardia* spp. *Carbohydr Res* **249**: 383-398, 1993
- 33 Dalziel TK: Thomas Kennedy Dalziel 1861-1924. Chronic interstitial enteritis. *Dis Colon Rectum* **32**: 1076-1078, 1989
- 34 Dannenberg AM, Jr.: Immune mechanisms in the pathogenesis of pulmonary tuberculosis. *Rev Infect Dis* **11 Suppl 2**: S369-378, 1989
- 35 Dow CT: Paratuberculosis and Type I diabetes: is this the trigger? *Med Hypotheses* **67**: 782-785, 2006

- 36 Dow CT, Ellingson JL: Detection of *Mycobacterium avium* ss. Paratuberculosis in Blau Syndrome Tissues. *Autoimmune Diseases* **2010**: 1-5, 2010
- 37 El-Zaatari FA, Osato MS, Graham DY: Etiology of Crohn's disease: the role of *Mycobacterium avium* paratuberculosis. *Trends Mol Med* **7**: 247-252, 2001
- 38 Ellingson JL, Bolin CA, Stabel JR: Identification of a gene unique to *Mycobacterium avium* subspecies paratuberculosis and application to diagnosis of paratuberculosis. *Mol Cell Probes* **12**: 133-142, 1998
- 39 Feller M, Huwiler K, Stephan R, Altpeter E, Shang A, Furrer H, Pfyffer GE, Jemmi T, Baumgartner A, Egger M: *Mycobacterium avium* subspecies paratuberculosis and Crohn's disease: a systematic review and meta-analysis. *Lancet Infect Dis* **7**: 607-613, 2007
- 40 Ferwerda G, Kullberg BJ, de Jong DJ, Girardin SE, Langenberg DML, van Crevel R, Ottenhoff THM, Van der Meer JWM, Netea MG: *Mycobacterium* paratuberculosis is recognized by Toll-like receptors and NOD2. *Journal of leukocyte biology* **82**: 1011-1018, 2007
- 41 Frank DN: *Mycobacterium avium* subspecies paratuberculosis and Crohn's disease. *Lancet Infect Dis* **8**: 345; author reply 345-346, 2008
- 42 Garcia Marin J, Chavez G, Aduriz J, Perez V, Juste R, Badiola J. Prevalence of paratuberculosis in infected goat flocks and comparison of different methods of diagnosis. *Proceedings of the 3rd International Colloquium on Paratuberculosis*, pp.157-167 1991

- 43 Garcia Marin J, Perez V, Badiola J. Prevalence and type of paratuberculosis lesions in sheep and their relation with the diagnosis by AGID test. Proceedings of the 3rd International Colloquium on Paratuberculosis, pp.172-180 1991
- 44 Giese SB, Ahrens P: Detection of Mycobacterium avium subsp. paratuberculosis in milk from clinically affected cows by PCR and culture. Vet Microbiol **77**: 291-297, 2000
- 45 Gonzalez J, Geijo MV, Garcia-Pariente C, Verna A, Corpa JM, Reyes LE, Ferreras MC, Juste RA, Garcia Marin JF, Perez V: Histopathological classification of lesions associated with natural paratuberculosis infection in cattle. J Comp Pathol **133**: 184-196, 2005
- 46 Goodger W, Collins M, Nordlund K, Eisele C, Pelletier J, Thomas CB, Sockett D: Epidemiologic study of on-farm management practices associated with prevalence of Mycobacterium paratuberculosis infections in dairy cattle. Journal of the American Veterinary Medical Association **208**: 1877, 1996
- 47 Groenendaal H, Nielen M, Jalvingh AW, Horst SH, Galligan DT, Hesselink JW: A simulation of Johne's disease control. Preventive Veterinary Medicine **54**: 225-245, 2002
- 48 Hanauer SB, Sandborn W: Management of Crohn's disease in adults. Am J Gastroenterol **96**: 635-643, 2001
- 49 Hansing B, Meeuwisse G: Regional enterocolitis (Crohn's disease). Clinical signs. Acta Paediatr Scand **60**: 104, 1971
- 50 Harris JE, Lammerding AM: Crohn's disease and Mycobacterium avium subsp. paratuberculosis: current issues. J Food Prot **64**: 2103-2110, 2001

- 51 Hawkins CC, Gold JW, Whimbey E, Kiehn TE, Brannon P, Cammarata R, Brown AE, Armstrong D: Mycobacterium avium complex infections in patients with the acquired immunodeficiency syndrome. *Ann Intern Med* **105**: 184-188, 1986
- 52 Hendrick SH, Duffield TF, Kelton DF, Leslie KE, Lissemore KD, Archambault M: Evaluation of enzyme-linked immunosorbent assays performed on milk and serum samples for detection of paratuberculosis in lactating dairy cows. *Journal of the American Veterinary Medical Association* **226**: 424-428, 2005
- 53 Hermon-Taylor J, Bull TJ, Sheridan JM, Cheng J, Stellakis ML, Sumar N: Causation of Crohn's disease by Mycobacterium avium subspecies paratuberculosis. *Canadian journal of gastroenterology= Journal canadien de gastroenterologie* **14**: 521, 2000
- 54 Herthnek D, Bolske G: New PCR systems to confirm real-time PCR detection of Mycobacterium avium subsp. paratuberculosis. *BMC Microbiol* **6**: 87, 2006
- 55 Hill AR, Premkumar S, Brustein S, Vaidya K, Powell S, Li PW, Suster B: Disseminated tuberculosis in the acquired immunodeficiency syndrome era. *Am Rev Respir Dis* **144**: 1164-1170, 1991
- 56 Hulten K, El-Zimaity HM, Karttunen TJ, Almashhrawi A, Schwartz MR, Graham DY, El-Zaatari FA: Detection of Mycobacterium avium subspecies paratuberculosis in Crohn's diseased tissues by in situ hybridization. *Am J Gastroenterol* **96**: 1529-1535, 2001
- 57 Hunnam JC, Wilson PR, Heuer C, Mackintosh CG, West DM, Clark RG: Histopathology of Grossly Normal Mesenteric Lymph Nodes of New Zealand Farmed Red Deer (Cervus elaphus) Including Identification of Lipopigment. *Vet Pathol*, 2010
- 58 Inderlied CB, Kemper CA, Bermudez LE: The Mycobacterium avium complex. *Clin Microbiol Rev* **6**: 266-310, 1993

- 59 Irengé LM, Walravens K, Govaerts M, Godfroid J, Rosseels V, Huygen K, Gala JL: Development and validation of a triplex real-time PCR for rapid detection and specific identification of *M. avium* sub sp. paratuberculosis in faecal samples. *Vet Microbiol* **136**: 166-172, 2009
- 60 Johnson-Ifearegulu Y, Kaneene JB: Distribution and environmental risk factors for paratuberculosis in dairy cattle herds in Michigan. *Am J Vet Res* **60**: 589-596, 1999
- 61 Johnson-Ifearegulu Y, Kaneene JB, Lloyd JW: Herd-level economic analysis of the impact of paratuberculosis on dairy herds. *J Am Vet Med Assoc* **214**: 822-825, 1999
- 62 Juste RA: Crohn's disease and ruminant farming. Got lactase? *Med Hypotheses* **75**: 7-13, 2010
- 63 Kawaji S, Taylor DL, Mori Y, Whittington RJ: Detection of *Mycobacterium avium* subsp. paratuberculosis in ovine faeces by direct quantitative PCR has similar or greater sensitivity compared to radiometric culture. *Vet Microbiol* **125**: 36-48, 2007
- 64 Kenneth J. Ryan CGR: *Sherris Medical Microbiology*, 5th ed. McGraw-Hill, New York, 2010
- 65 Kuehnelt MP, Goethe R, Habermann A, Mueller E, Rohde M, Griffiths G, Valentin-Weigand P: Characterization of the intracellular survival of *Mycobacterium avium* ssp. paratuberculosis: phagosomal pH and fusogenicity in J774 macrophages compared with other mycobacteria. *Cell Microbiol* **3**: 551-566, 2001
- 66 Larsen AB, Merkal RS, Vardaman TH: Survival time of *Mycobacterium paratuberculosis*. *Am J Vet Res* **17**: 549-551, 1956

- 67 Loftus EV, Jr., Schoenfeld P, Sandborn WJ: The epidemiology and natural history of Crohn's disease in population-based patient cohorts from North America: a systematic review. *Aliment Pharmacol Ther* **16**: 51-60, 2002
- 68 Mahaisavariya P, Chaiprasert A, Khemngern S, Manonukul J, Gengviniij N, Ubol PN, Pinitugsorn S: Nontuberculous mycobacterial skin infections: clinical and bacteriological studies. *J Med Assoc Thai* **86**: 52-60, 2003
- 69 Massone AR, Martin AA, Ibargoyen GS, Gimeno EJ: Immunohistochemical methods for the visualization of *Mycobacterium paratuberculosis* in bovine tissues. *Zentralbl Veterinarmed B* **37**: 251-253, 1990
- 70 McClure HM, Chiodini RJ, Anderson DC, Swenson RB, Thayer WR, Coutu JA: *Mycobacterium paratuberculosis* infection in a colony of stumptail macaques (*Macaca arctoides*). *J Infect Dis* **155**: 1011-1019, 1987
- 71 Merkal RS, Larsen AB: Clofazimine treatment of cows naturally infected with *Mycobacterium paratuberculosis*. *Am J Vet Res* **34**: 27-28, 1973
- 72 Murray CJL SK, Rouillon A: *Disease Control Priorities in Developing Countries*, ed. Jamison DaM, WH. Oxford University Press for the World Bank, New York, 1992
- 73 Nacy C, Buckley M: *Mycobacterium avium paratuberculosis*: infrequent human pathogen or public health threat. *A report from the American Academy of Microbiology*: 1-37, 2008
- 74 Nalubamba KS, Gossner AG, Dalziel RG, Hopkins J: Differential expression of pattern recognition receptors in sheep tissues and leukocyte subsets. *Veterinary immunology and immunopathology* **118**: 252-262, 2007

- 75 Naser SA, Collins MT, Crawford JT, Valentine JF: Culture of Mycobacterium avium subspecies paratuberculosis(MAP) from the Blood of Patients with Crohn's disease: A Follow-Up Blind Multi Center Investigation. *Open Inflammation Journal* **2**: 22-23, 2009
- 76 Naser SA, Ghobrial G, Romero C, Valentine JF: Culture of Mycobacterium avium subspecies paratuberculosis from the blood of patients with Crohn's disease. *Lancet* **364**: 1039-1044, 2004
- 77 Naser SA, Schwartz D, Shafran I: Isolation of Mycobacterium avium subsp paratuberculosis from breast milk of Crohn's disease patients. *Am J Gastroenterol* **95**: 1094-1095, 2000
- 78 National Research Council (U.S.). Committee on Diagnosis and Control of Johne's Disease.: Diagnosis and control of Johne's disease pp. xiv, 229 p. National Academies Press, Washington, D.C., 2003
- 79 Nielsen SS, Toft N: Age-specific characteristics of ELISA and fecal culture for purpose-specific testing for paratuberculosis. *Journal of dairy science* **89**: 569-579, 2006
- 80 Nielsen SS, Toft N: Ante mortem diagnosis of paratuberculosis: A review of accuracies of ELISA, interferon-[gamma] assay and faecal culture techniques. *Veterinary microbiology* **129**: 217-235, 2008
- 81 Ooi WW, Moschella SL: Update on leprosy in immigrants in the United States: status in the year 2000. *Clin Infect Dis* **32**: 930-937, 2001
- 82 Ott SL, Wells SJ, Wagner BA: Herd-level economic losses associated with Johne's disease on US dairy operations. *Prev Vet Med* **40**: 179-192, 1999
- 83 Palenque E: Skin disease and nontuberculous atypical mycobacteria. *Int J Dermatol* **39**: 659-666, 2000

- 84 Pattisapu R.J. Ganadharam PAJ: Mycobacteria I: Basic Aspects. *In*: Chapman & Hall Medical Microbiology Series, p. 390. International Thomson Publishing, New York, 1998
- 85 Perez V, Garcia Marin JF, Badiola JJ: Description and classification of different types of lesion associated with natural paratuberculosis infection in sheep. *J Comp Pathol* **114**: 107-122, 1996
- 86 Pierce ES: Possible transmission of *Mycobacterium avium* subspecies paratuberculosis through potable water: lessons from an urban cluster of Crohn's disease. *Gut Pathog* **1**: 17, 2009
- 87 Plain KM, Purdie AC, Begg DJ, de Silva K, Whittington RJ: Toll-like receptor (TLR) 6 and TLR1 differentiation in gene expression studies of Johne's disease. *Veterinary immunology and immunopathology* **137**: 142-148, 2010
- 88 Plante Y, Remenda BW, Chelack BJ, Haines DM: Detection of *Mycobacterium paratuberculosis* in formalin-fixed paraffin-embedded tissues by the polymerase chain reaction. *Can J Vet Res* **60**: 115-120, 1996
- 89 Pott J, Basler T, Duerr CU, Rohde M, Goethe R, Hornef MW: Internalization-dependent recognition of *Mycobacterium avium* ssp. paratuberculosis by intestinal epithelial cells. *Cellular microbiology* **11**: 1802-1815, 2009
- 90 Prince DS, Peterson DD, Steiner RM, Gottlieb JE, Scott R, Israel HL, Figueroa WG, Fish JE: Infection with *Mycobacterium avium* complex in patients without predisposing conditions. *N Engl J Med* **321**: 863-868, 1989
- 91 Qual DA, Kaneene JB, Varty TJ, Miller R, Thoen CO: Lack of association between the occurrence of Crohn's disease and occupational exposure to dairy and beef cattle herds

- infected with *Mycobacterium avium* subspecies *paratuberculosis*. *J Dairy Sci* **93**: 2371-2376, 2010
- 92 Ravva SV, Stanker LH: Real-time quantitative PCR detection of *Mycobacterium avium* subsp. *paratuberculosis* and differentiation from other mycobacteria using SYBR Green and TaqMan assays. *J Microbiol Methods* **63**: 305-317, 2005
- 93 Rosseels V, Roupie V, Zinniel D, Barletta RG, Huygen K: Development of luminescent *Mycobacterium avium* subsp. *paratuberculosis* for rapid screening of vaccine candidates in mice. *Infection and immunity* **74**: 3684, 2006
- 94 Rossiter CA, Burhans WS: Farm-specific approach to paratuberculosis (Johne's disease) control. *The Veterinary clinics of North America Food animal practice* **12**: 383, 1996
- 95 Rowbotham DS, Mapstone NP, Trejdosiewicz LK, Howdle PD, Quirke P: *Mycobacterium paratuberculosis* DNA not detected in Crohn's disease tissue by fluorescent polymerase chain reaction. *Gut* **37**: 660-667, 1995
- 96 Ruiz-Larrañaga O, Manzano C, Iriondo M, Garrido J, Molina E, Vazquez P, Juste R, Estonba A: Genetic variation of toll-like receptor genes and infection by *Mycobacterium avium* ssp. *paratuberculosis* in Holstein-Friesian cattle. *Journal of dairy science* **94**: 3635-3641, 2011
- 97 Sanftleben P: Quest continues for fast, reliable test for bovine paratuberculosis. *J Am Vet Med Assoc* **197**: 299-305, 1990
- 98 Sartor RB: Mechanisms of disease: pathogenesis of Crohn's disease and ulcerative colitis. *Nat Clin Pract Gastroenterol Hepatol* **3**: 390-407, 2006
- 99 Saunders LZ: A biographical history of veterinary pathology pp. xviii, 589 p. Allen Press, Lawrence, Kan., 1996

- 100 Schmidt A, Weber OF: In memoriam of Rudolf Virchow: a historical retrospective including aspects of inflammation, infection and neoplasia. *Contrib Microbiol* **13**: 1-15, 2006
- 101 Schonenbrucher H, Abdulmawjood A, Failing K, Bulte M: New triplex real-time PCR assay for detection of *Mycobacterium avium* subsp. *paratuberculosis* in bovine feces. *Appl Environ Microbiol* **74**: 2751-2758, 2008
- 102 Schwartz D, Shafran I, Romero C, Piromalli C, Biggerstaff J, Naser N, Chamberlin W, Naser SA: Use of short-term culture for identification of *Mycobacterium avium* subsp. *paratuberculosis* in tissue from Crohn's disease patients. *Clin Microbiol Infect* **6**: 303-307, 2000
- 103 Scollard DM, Gillis TP, Williams DL: Polymerase chain reaction assay for the detection and identification of *Mycobacterium leprae* in patients in the United States. *Am J Clin Pathol* **109**: 642-646, 1998
- 104 Sechi LA, Mura M, Tanda F, Lissia A, Solinas A, Fadda G, Zanetti S: Identification of *Mycobacterium avium* subsp. *paratuberculosis* in biopsy specimens from patients with Crohn's disease identified by in situ hybridization. *J Clin Microbiol* **39**: 4514-4517, 2001
- 105 Shafran I, Kugler L, El-Zaatari FA, Naser SA, Sandoval J: Open clinical trial of rifabutin and clarithromycin therapy in Crohn's disease. *Dig Liver Dis* **34**: 22-28, 2002
- 106 Sherman DM, Markham RJ, Bates F: Agar gel immunodiffusion test for diagnosis of clinical paratuberculosis in cattle. *J Am Vet Med Assoc* **185**: 179-182, 1984
- 107 Sigur-Dardottir OG, Press CM, Evensen O: Uptake of *Mycobacterium avium* subsp. *paratuberculosis* through the distal small intestinal mucosa in goats: an ultrastructural study. *Vet Pathol* **38**: 184-189, 2001

- 108 Singh S, Singh P, Singh M, Singh A, Sohal J: Therapeutic potential of Johne's disease vaccine: A follow up post vaccination study in a goatherd of endangered Jamunapari breed, naturally infected with *Mycobacterium avium* subspecies paratuberculosis. *International Journal of Livestock Production* **2**: 192-204, 2011
- 109 Singh SV, Singh PK, Singh AV, Sohal JS, Sharma MC: Therapeutic Effects of a New "Indigenous Vaccine" Developed Using Novel Native "Indian Bison Type" Genotype of *Mycobacterium avium* Subspecies paratuberculosis for the Control of Clinical Johne's Disease in Naturally Infected Goatherds in India. *Veterinary Medicine International* **2010**: 1-8, 2010
- 110 Sisto M, Cucci L, D'Amore M, Dow TC, Mitolo V, Lisi S: Proposing a relationship between *Mycobacterium avium* subspecies paratuberculosis infection and Hashimoto's thyroiditis. *Scand J Infect Dis* **42**: 787-790, 2010
- 111 Smedh K, Olaison G, Franzen L, Sjodahl R: Endoscopic and external bowel changes and histopathology in patients with Crohn's disease. *Br J Surg* **82**: 191-194, 1995
- 112 Snider DE, Jr., Long MW, Cross FS, Farer LS: Six-months isoniazid-rifampin therapy for pulmonary tuberculosis. Report of a United States Public Health Service Cooperative Trial. *Am Rev Respir Dis* **129**: 573-579, 1984
- 113 Souza CD, Evanson OA, Sreevatsan S, Weiss DJ: Cell membrane receptors on bovine mononuclear phagocytes involved in phagocytosis of *Mycobacterium avium* subsp paratuberculosis. *American journal of veterinary research* **68**: 975-980, 2007
- 114 St-Jean G, Jernigan AD: Treatment of *Mycobacterium* paratuberculosis infection in ruminants. *Vet Clin North Am Food Anim Pract* **7**: 793-804, 1991

- 115 St Jean G: Treatment of clinical paratuberculosis in cattle. *Vet Clin North Am Food Anim Pract* **12**: 417-430, 1996
- 116 Stabel J: Host responses to *Mycobacterium avium* subsp. paratuberculosis: a complex arsenal. *Animal Health Research Reviews* **7**: 61-70, 2006
- 117 Stabel J: Transitions in immune responses to *Mycobacterium paratuberculosis*. *Veterinary microbiology* **77**: 465-473, 2000
- 118 Stabel J, Wells S, Wagner B: Relationships between fecal culture, ELISA, and bulk tank milk test results for Johne's disease in US dairy herds. *Journal of dairy science* **85**: 525-531, 2002
- 119 Stabel JR: Cytokine secretion by peripheral blood mononuclear cells from cows infected with *Mycobacterium paratuberculosis*. *Am J Vet Res* **61**: 754-760, 2000
- 120 Stabel JR: Production of gamma-interferon by peripheral blood mononuclear cells: an important diagnostic tool for detection of subclinical paratuberculosis. *J Vet Diagn Invest* **8**: 345-350, 1996
- 121 Stabel JR, Ackermann MR, Goff JP: Comparison of polyclonal antibodies to three different preparations of *Mycobacterium paratuberculosis* in immunohistochemical diagnosis of Johne's disease in cattle. *J Vet Diagn Invest* **8**: 469-473, 1996
- 122 Streeter RN, Hoffsis GF, Bech-Nielsen S, Shulaw WP, Rings DM: Isolation of *Mycobacterium paratuberculosis* from colostrum and milk of subclinically infected cows. *Am J Vet Res* **56**: 1322-1324, 1995
- 123 Stringer L, Wilson P, Heuer C, Hunnam J, Mackintosh C: Effect of vaccination and natural infection with *Mycobacterium avium* subsp. paratuberculosis on specificity of diagnostic

- tests for bovine tuberculosis in farmed red deer (*Cervus elaphus*). *New Zealand Veterinary Journal* **59**: 218-224, 2011
- 124 Subharat S, Shu D, de Lisle GW, Buddle BM, Wedlock DN: Altered patterns of toll-like receptor gene expression in cull cows infected with *Mycobacterium avium* subsp. *paratuberculosis*. *Vet Immunol Immunopathol*, 2011
- 125 Sweeney RW: Transmission of paratuberculosis. *Vet Clin North Am Food Anim Pract* **12**: 305-312, 1996
- 126 Sweeney RW, Whitlock RH, McAdams SC: Comparison of three DNA preparation methods for real-time polymerase chain reaction confirmation of *Mycobacterium avium* subsp. *paratuberculosis* growth in an automated broth culture system. *J Vet Diagn Invest* **18**: 587-590, 2006
- 127 Taddei R, Barbieri I, Pacciarini ML, Fallacara F, Belletti GL, Arrigoni N: *Mycobacterium porcinum* strains isolated from bovine bulk milk: implications for *Mycobacterium avium* subsp. *paratuberculosis* detection by PCR and culture. *Vet Microbiol* **130**: 338-347, 2008
- 128 Taddei S, Robbi C, Cesena C, Rossi I, Schiano E, Arrigoni N, Vicenzoni G, Cavarani S: Detection of *Mycobacterium Avium* Subsp. *Paratuberculosis* in Bovine Fecal Samples: Comparison of Three Polymerase Chain Reaction—Based Diagnostic Tests with a Conventional Culture Method. *Journal of Veterinary Diagnostic Investigation* **16**: 503, 2004
- 129 Tasara T, Stephan R: Development of an F57 sequence-based real-time PCR assay for detection of *Mycobacterium avium* subsp. *paratuberculosis* in milk. *Appl Environ Microbiol* **71**: 5957-5968, 2005

- 130 Tavoranpanich S, Gardner IA, Anderson RJ, Shin S, Whitlock RH, Fyock T, Adaska JM, Walker RL, Hietala SK: Evaluation of microbial culture of pooled fecal samples for detection of *Mycobacterium avium* subsp paratuberculosis in large dairy herds. *Am J Vet Res* **65**: 1061-1070, 2004
- 131 Taylor DL, Zhong L, Begg DJ, de Silva K, Whittington RJ: Toll-like receptor genes are differentially expressed at the sites of infection during the progression of Johne's disease in outbred sheep. *Veterinary immunology and immunopathology* **124**: 132-151, 2008
- 132 Thorel MF: Review of the occurrence of mycobactin dependence among mycobacteria species. *Ann Rech Vet* **15**: 405-409, 1984
- 133 Thorne J, Hardin L: Estimated prevalence of paratuberculosis in Missouri, USA cattle. *Preventive Veterinary Medicine* **31**: 51-57, 1997
- 134 Tufariello JM, Chan J, Flynn JL: Latent tuberculosis: mechanisms of host and bacillus that contribute to persistent infection. *Lancet Infect Dis* **3**: 578-590, 2003
- 135 Valentin-Weigand P, Goethe R: Pathogenesis of *Mycobacterium avium* subspecies paratuberculosis infections in ruminants: still more questions than answers. *Microbes Infect* **1**: 1121-1127, 1999
- 136 Valentin-Weigand P, Moriarty K: *Mycobacterium paratuberculosis* binds fibronectin. *Research in microbiology* **143**: 75-79, 1992
- 137 Vary PH, Andersen PR, Green E, Hermon-Taylor J, McFadden JJ: Use of highly specific DNA probes and the polymerase chain reaction to detect *Mycobacterium paratuberculosis* in Johne's disease. *J Clin Microbiol* **28**: 933-937, 1990

- 138 West G, Agbo M, Willeberg P, Ruppanner R, Aalund O, Behymer D: Paratuberculosis [Mycobacterium paratuberculosis] in California dairy goats. *California Veterinarian* **33**, 1979
- 139 Whittington RJ, Reddacliff L, Marsh I, Saunders V: Detection of Mycobacterium avium subsp paratuberculosis in formalin-fixed paraffin-embedded intestinal tissue by IS900 polymerase chain reaction. *Aust Vet J* **77**: 392-397, 1999
- 140 Williams ES, Snyder SP, Martin KL: Pathology of spontaneous and experimental infection of North American wild ruminants with Mycobacterium paratuberculosis. *Vet Pathol* **20**: 274-290, 1983
- 141 Woo SR, Heintz JA, Albrecht R, Barletta RG, Czuprynski CJ: Life and death in bovine monocytes: the fate of Mycobacterium avium subsp. paratuberculosis. *Microb Pathog* **43**: 106-113, 2007

Evaluation of a Commercial Paratuberculosis Real-Time Quantitative Polymerase Chain Reaction Assay on Formalin-Fixed Paraffin-Embedded Tissues for the Detection of *Mycobacterium avium* subspecies *paratuberculosis*

ABSTRACT

At necropsy, diagnosis of Johne's disease (caused in ruminants by infection with *Mycobacterium avium* ss. *paratuberculosis* (MAP)) is commonly confirmed through microscopic examination of stained sections of formalin-fixed, paraffin embedded (FFPE) tissues. This study evaluated a commercial paratuberculosis real-time quantitative PCR (qPCR) assay targeting MAP specific heat shock protein X (MAP *hspX*) applied to FFPE tissues.

Eighty-five FFPE tissue blocks from 70 ruminants diagnosed with Johne's disease by independent laboratories (positive clinical cases) were obtained to make 25µm scroll samples and processed by a simple freeze/boil DNA extraction method and tested using two commercial paratuberculosis real-time quantitative PCR protocols, one targeting the MAP specific *hspX* gene and the other targeting the MAP specific insertion sequence 900 (IS900) gene. Twenty-one FFPE tissue blocks from 8 known uninfected animals combined with thirteen FFPE tissue blocks from 6 non-ruminant animals diagnosed with non-paratuberculosis mycobacterial diseases were used as negative clinical cases and tested by the MAP *hspX* qPCR protocol.

Scrolls from negative clinical cases (34 FFPE tissue blocks) were all qPCR negative (Specificity = 100%). Scrolls from the positive clinical cases (85 FFPE tissue blocks) were used to determine the sensitivity for the MAP *hspX* qPCR assay protocol which ranged from 92%-96%. Compared to the commercial IS900 qPCR assay, 76 of the 81 FFPE tissues were qPCR positive (sensitivity = 94%). Compared to fecal culture positive and IS900 qPCR results, 22 of 24 FFPE tissues were qPCR positive (sensitivity = 92%). Compared to positive histopathology with acid fast bacteria, 73 of 79 of the scrolls were qPCR positive (sensitivity = 92%). Compared

to positive histopathology with acid fast bacteria combined with the IS900 qPCR results, 73 of 76 of the scrolls were qPCR positive (sensitivity = 96%). The MAP *hspX* qPCR results from two different light-detecting thermocycler instruments were compared for uniformity and the results highly correlated (Pearson's  $r = 0.84$ ,  $p < 0.0001$ ,  $n = 117$ ) and agreement for interpretation of results was almost perfect (Cohen's  $k = 0.81$ ).

This protocol expands the diagnostic value of FFPE tissues, provides specific confirmation of MAP infection in multiple species, and uses widely available and easily transported diagnostic samples. The approach is useful for retrospective studies of formalin-fixed paraffin-embedded tissues or in diagnostic cases where histopathology is inconclusive, or when fresh tissues are not available for culture.

## **Introduction:**

*Mycobacterium avium* subspecies *paratuberculosis* (MAP) infection in ruminants causes Johne's disease, a fatal chronic inflammatory enteric disease. While usually infected in the first months of life, the majority of ruminants do not progress to clinical disease (emaciation, diarrhea in some species) for several years.<sup>17</sup> A common gross lesion in clinically ill ruminants (especially cattle) in later stages of Johne's disease is segmental thickening of the distal small intestine with a corrugated mucosal surface.<sup>2,4,11</sup> Microscopic intestinal lesions are characterized by focal, multifocal, or diffuse mucosal infiltration by macrophages and multinucleate giant cells that may contain few (paucibacillary) or myriad (multibacillary) acid-fast rods.<sup>2,4,7,11</sup> The adjacent lymphoid tissue (Peyer's patches) and mesenteric lymph node chain may be infiltrated by similar inflammatory cells with intracellular MAP.<sup>2,4,11</sup> In earlier stages of infection, gross lesions may be absent and acid-fast organisms may be so few as to be undetectable.<sup>7</sup>

International surveillance has confirmed that Johne's disease is a global agricultural problem. In the United States the dairy industry loses an estimated \$200-250 million annually due to the infection with an estimated 68.1% herd-level prevalence.<sup>9,10</sup> The infection is of concern for other domestic and free-ranging ruminants such as goats, sheep, deer, and bison as well.<sup>1,4,8,11</sup>

Both for animal health and economic reasons, efficient, affordable and accurate surveillance tools are necessary for effective MAP infection control. Standard Johne's disease ante-mortem diagnostic testing includes antibody-dependent assays (milk and serum ELISAs) and isolation and identification of the organism from fresh tissues, fecal or environmental sample or direct fecal PCR. Fecal and environmental samples can be pooled with limited loss of sensitivity to establish the infection status of a premise.<sup>16</sup> Post-mortem diagnostics include gross

and microscopic examination of pertinent tissues (i.e. ileum, mesenteric lymph nodes), plus isolation of MAP from these same tissues by culture.

The development of PCR assays for the detection of MAP-specific genetic sequences such as the insertion sequence 900 (IS900)<sup>13,18</sup> and MAP *hspX*<sup>6</sup> has expanded the repertoire of diagnostic targets for Johne's disease testing. Direct fecal PCR is now an accepted diagnostic assay for the National Voluntary Bovine Johne's Disease Control Program in the United States.<sup>3</sup> A recently developed commercial real-time PCR assay<sup>a</sup> targeting the MAP *hspX* gene is now commonly used to detect MAP in bovine fecal samples. This assay takes less time than traditional PCR, because gel electrophoresis is not required. Results are based on cycle threshold (Ct) values provided by a real-time PCR light-detecting thermocycler.

The formalin-fixed and paraffin-embedded (FFPE) technique is one of the most common preservation and archiving techniques for tissues collected by biopsy or at necropsy. FFPE tissue blocks contain a potential wealth of epidemiologic data: virtually all diagnostic laboratories use the method, the tissue blocks are usually accompanied by informative case histories, they are retained for years, and sampling rarely exhausts the diagnostic material they contain.<sup>8</sup> The use of a simple freeze/boil DNA extraction technique combined with conventional MAP IS900 PCR testing has been reported to produce consistent positive results.<sup>19</sup> With advances in DNA extraction and commercially available real-time quantitative PCR kits, it is now feasible for any laboratory to obtain Johne's disease diagnostic information via qPCR from FFPE tissues. The purpose of this study was to evaluate the performance of a commercial real-time quantitative PCR assay on FFPE tissues.

## Materials and Methods

To evaluate the performance of a commercial real-time quantitative PCR assay applied to FFPE tissues, two sets of case material were used. They consisted of 85 tissue blocks from 70 ruminants (45-bovine, 8-ovine, and 17-caprine) assigned a final diagnosis of Johne's disease by a veterinary diagnostic laboratory unaffiliated with the study. Negative controls were 21 tissue blocks from eight young animals from MAP-negative herds dying from causes unrelated to mycobacteriosis or gastrointestinal disease and 13 tissue blocks from 6 non-ruminant animals diagnosed with a non-paratuberculosis mycobacterial disease (**Table 2.1**). The FFPE tissue blocks from the 8 known uninfected animals were of small intestine and mesenteric lymph nodes and were animals that were diagnosed with non-gastrointestinal disease at necropsy. The FFPE tissue blocks from the 6 non-ruminant animals diagnosed with non-paratuberculosis mycobacterial disease contained sections of granulomatous inflammation with intra-lesional acid-fast bacteria.

Each animal representing a Johne's disease case was a clinically ill (emaciated) adult from a herd with prior cases of Johne's disease, and was either fecal culture positive (n=28, **Table 2.2**) or had gross and histopathologic lesions compatible with Johne's disease (granulomatous lymphadenitis/enteritis n=85, **Table 2.3**) according to the laboratory contributing the tissue blocks.

### Johne's disease histopathology:

The first portion of the study entailed two pathologists independently examining and assigning a score of 1 for the presence of granulomatous inflammation or 0 for no granulomatous inflammation present in sections from the tissue blocks. The FFPE tissue blocks were prepared by standard protocols (fixed in neutral buffered formalin, processed with xylene and alcohol and

embedded in paraffin) and were coded to conceal whether they were positive or negative samples. Each block contained at least one tissue relevant for Johne's disease diagnosis (small intestine or mesenteric lymph node). A 5 µm section was sliced by microtome from each FFPE tissue block, fixed on a glass slide and stained with hematoxylin and eosin (H&E) for microscopic assessment of granulomatous inflammation. Granulomatous inflammation consistent with Johne's disease was seen on all slides prepared from the Johne's disease tissue blocks according to both pathologists (n = 85).

#### FFPE Scroll sampling and DNA extraction:

For MAP qPCR testing, 25 µm scrolls were cut by microtome from each of the 85 case tissue blocks and the 21 negative control tissue blocks. To prevent cross-contamination, the microtome blade and forceps were wiped clean with a 10% bleach (sodium hypochlorite) solution between each block. DNA was extracted by the boil-freeze method as described previously.<sup>19</sup> Briefly, scrolls were transferred to sterile 1.5 ml screw-cap graduated conical tubes<sup>e</sup> and centrifuged for 1 minute at 24,000 x g. To each of the pelleted tissue scrolls, 200 µl of 0.5% Tween 20 was added, and the sample tubes were placed in a heat block at 100°C for 10 minutes. The tubes were then immersed in liquid nitrogen for 15-20 seconds to snap-freeze the contents. The boil/snap-freeze steps were repeated once, followed by an additional boil step. The tubes were then centrifuged for 20 minutes at 850 x g. After centrifugation, the resultant liquid was transferred to coded sterile 1.5ml microcentrifuge tube<sup>d</sup> and frozen at -20°C for storage.

#### MAP qPCR testing:

The second section of the study entailed testing the extracted DNA for MAP *hspX* and IS900 according to the two commercial qPCR kit manufacturers' instructions.<sup>a,g</sup> All DNA extracts were run on a BioRad iCycler<sup>b</sup> with a positive result for MAP *hspX* defined as Ct ≤ 38

(the cut-off established by the manufacturer based on validations with bovine fecal samples). The DNA extracts from the FFPE tissue blocks of the 85 Johne's disease cases were also tested using the commercial IS900 based qPCR assay<sup>g</sup> using the BioRad iCycler<sup>b</sup> thermocycler and results were recorded as positive if the qPCR Ct result was < 45 for the FAM-490 fluorescent dye as per the manufacturer's interpretation instructions.

## Results

Specificity was calculated to be 100% as the 34 tissue blocks from the eight uninfected animals and 6 non-ruminant animals diagnosed with a non-paratuberculosis mycobacterial disease each produced Ct values > 38 using the MAP *hspX* gene as the target, interpreted as negative.

Of 85 Johne's disease cases defined by external laboratories based on the highly diagnostic gross and microscopic lesions, positive MAP IS900 qPCR results were obtained for 81 of the samples and positive MAP *hspX* qPCR results were obtained for 76 samples, with 4 samples being negative by both qPCR assays (Sensitivity **93.8%**)(Table 2.4). Of the 85 FFPE tissue samples 28 came from animals with positive MAP fecal cultures. Twenty four of these samples were IS900 qPCR positive and of these, 22 were positive by the MAP *hspX* qPCR assay (Sensitivity **91.7%**). Comparing qPCR results to histopathology, microscopic examination identified 79 cases with acid-fast bacteria present, while 73 were positive by the MAP *hspX* qPCR assay (Sensitivity **92.4%**). Seventy-six FFPE tissue blocks had acid-fast bacteria present by histopathology and were positive by IS900 qPCR testing, and 73 of these blocks tested positive by the MAP *hspX* qPCR assay (Sensitivity **96.1%**).

All of the case definition and clinical samples (DNA extracted from 85 cases), and most of the negative control tissue blocks (32/34) were also run on a Stratagene Mx3005p<sup>c</sup> real-time PCR instrument to assess result uniformity across light-detecting thermocycle instruments. The results were highly correlated (Pearson's  $r = 0.84$ ,  $n = 117$ ,  $p < 0.0001$ ) (**Figure 2.1**). There was near perfect agreement between the Stratagene Mx3005p<sup>c</sup> and BioRad iCycler<sup>b</sup> result interpretations (Cohen's  $k = 0.81$ ,  $n = 117$ ). All statistics were calculated using JMP® 9.0 statistical software.<sup>f</sup>

## **Discussion & Conclusion**

While microscopic detection of acid fast bacteria combined with IS900 qPCR was associated with the highest MAP *hspX* qPCR sensitivity (96%), there were three samples that were positive for acid-fast bacteria by histopathology but were negative by both IS900 and MAP *hspX* qPCR testing. It is possible that the acid-fast organisms seen were not MAP, but were instead a different mycobacterial organism (e.g. *Mycobacterium avium* ss *avium*) meaning the initial diagnosis of Johne's disease was incorrect (as microscopic evaluation alone cannot speciate the mycobacterial organisms seen). Of the 85 FFPE tissue blocks, 81 tested positive by the IS900 qPCR assay compared to 79 testing positive by the MAP *hspX* qPCR assay. This may be related to the number of target genes copies in the genome, with 14-20 IS900 gene copies in the MAP genome compared to just one MAP *hspX* gene copy in the MAP genome. Negative MAP *hspX* qPCR results were found for 9 ruminants (7-bovine, 2-ovine) diagnosed with Johne's disease by the veterinary diagnostic laboratory that supplied the samples. In this study, eight of thirteen FFPE tissues from with lesions highly diagnostic for Johne's disease but had scant or no

visible acid-fast organisms (acid fast score 0-1) were confirmed as cases of Johne's disease via the MAP *hspX* qPCR method.

Another possible explanation for the negative qPCR results obtained from the Johne's disease positive case material may have been due to tissues' excessive exposure to formalin, DNA extraction methods, or to an unknown PCR inhibitory component. Age of the FFPE tissues (time spent embedded in paraffin) did not affect the results (positive vs. negative) of the commercial qPCR assay as all of the FFPE tissues that were over 10 years (embedded in paraffin before 2001, n = 10) had positive results. The oldest FFPE tissues were embedded in 1996.

Extraction of DNA from FFPE tissue sections by the boil-freeze method is rapid, simple and does not require volatile solvents such as xylene.<sup>12,19</sup> DNA extractions can be processed per batch with this diagnostic platform, and confirmation of MAP infection can be made in varied species. The approach provides additional evidence for a diagnosis of Johne's disease at a reasonable cost, particularly in paucibacillary cases when additional sectioning, staining and scrutiny might have been required. With this assay a laboratory may provide an organism-specific diagnosis (vs. only "acid-fast organisms seen") by identifying MAP specific DNA consistent with Johne's disease infection. The approach is useful when fresh tissue is not available for examination or culture, as may occur in wildlife diagnostics. The sensitivity of this approach, as with all Johne's disease diagnostics, is affected by the stage of infection at necropsy and the types of tissues selected for analysis. Tissues tested must be those known to harbor the MAP organism such as ileum, jejunum, or mesenteric lymph nodes.

This is the first commercially available qPCR assay to target the MAP *hspX* gene (vs. the MAP *IS900* gene which is potentially less specific given the *IS900*-like homolog genes described in distantly related Mycobacteria such as *Mycobacterium porcinum* in previous

reports).<sup>15</sup> To quantify precisely the method's diagnostic specificity, future evaluation of the diagnostic method should include FFPE tissue scrolls from a statistically significant number of known uninfected animals. Sensitivity could be determined with paucibacillary infections and samples from known infected animals with autolyzed tissues. Tissue samples as old as twenty years still tested positive. There was no correlation between age of tissue and qPCR results, though this could be a factor. Of additional interest might be inclusion of an internal amplification control element to monitor false-negative results due to qPCR inhibition. Because  $\beta$ -glycosidic bonds in purine bases are hydrolyzed at pH 4, care should be taken to ensure that formalin is buffered to limit MAP DNA degradation.<sup>5,14,20</sup>

Because FFPE tissue blocks are archived for at least several years, the MAP *hspX* qPCR supports retrospective studies investigating the severity, extent and distribution of MAP infections over time in different tissues, varied animal species (including humans), and from diverse geographic populations.

In conclusion, because of the strong sensitivity of these paratuberculosis qPCR assays on FFPE tissues, these tests can serve a valuable role in diagnostic pathology & clinical microbiology. With such strong sensitivities, these diagnostic tests would be useful in research medicine investigating differences of paratuberculosis amongst populations (geographical, breed, prevalence, therapeutic, etc.).

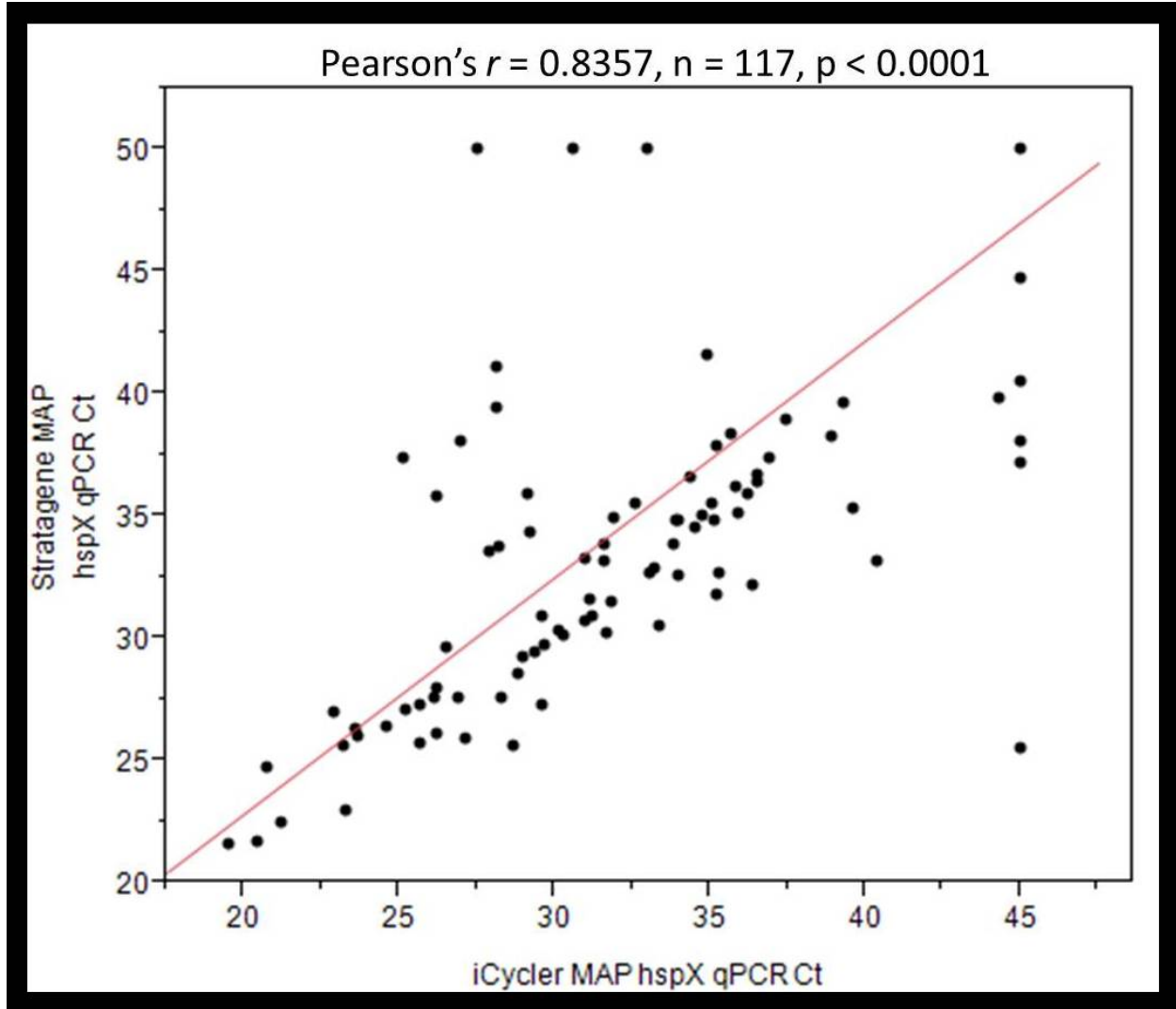
### **Sources and manufacturers**

- a. VetAlert<sup>TM</sup>, Tetracore® Inc. Rockville, MD
- b. iCycler, BioRad Laboratories Inc., Hercules, CA
- c. Stratagene Mx3005p, Agilent Technologies Inc., Santa Clara, CA

- d. 1.5 ml microcentrifuge tube, Sigma-Aldrich Inc., St. Louis, MO
- e. 1.5 ml screw top microtube, Sarstedt, Aktiengesellschaft & Co., Germany
- f. JMP® 8.0 Statistical software, SAS Institute Inc., Cary, NC
- g. AdiaVet ParaTB™, Adiagene® Inc., Paris France

## Figures

**Figure 2.1:** Correlation between BioRad iCycler and Stratagene Mx3005p light detecting thermocycler MAP *hspX* qPCR results.



## Tables

**Table 2.1:** Negative cases

Negative cases, species, tissue, Acid Fast Score (AFS), quantitative polymerase chain reaction results (qPCR), interpretation of iCycler MAP hspX qPCR assay per manufacturer							
Block ID#	Species	Tissues	AFS (0-4) Pathologist 1	AFS (0-4) Pathologist 2	qPCR 1	interp.	qPCR 2
VT Neg 4	Bovine	ileum & abscess wall	0	0	No Ct	Neg	No Ct
VT Neg 8	Bovine	si & abomasum	0	0	No Ct	Neg	No Ct
VT Neg 10	Bovine	si & abomasum	0	0	No Ct	Neg	No Ct
VT Neg 13	Bovine	colon, si, abomasum	0	0	No Ct	Neg	No Ct
VT Neg 14	Bovine	small intestine	0	0	No Ct	Neg	No Ct
VT Neg 15	Ovine	small intestine, rumen	0	0	No Ct	Neg	38.1
VT Neg 16	Ovine	small intestine	0	0	No Ct	Neg	No Ct
VT Neg 17	Ovine	small intestine	0	0	No Ct	Neg	No Ct
Wisc Neg 12	Bison	small intestine	0	0	No Ct	Neg	No Ct
Wisc Neg 6	Bison	small intestine	0	0	No Ct	Neg	No Ct
Wisc Neg 24	Bison	MLN	0	0	No Ct	Neg	No Ct
Wisc Neg 18	Bison	small intestine	0	0	No Ct	Neg	No Ct
Wisc Neg 30	Bison	small intestine	0	0	No Ct	Neg	No Ct
Wisc Neg 15	Swine	MLN	0	0	No Ct	Neg	No Ct
Wisc Neg 13	Swine	small intestine	0	0	No Ct	Neg	No Ct
Wisc Neg 14	Swine	MLN	0	0	No Ct	Neg	No Ct
Wisc Neg 20	Swine	small intestine	0	0	No Ct	Neg	No Ct
Wisc Neg 21	Swine	MLN	0	0	No Ct	Neg	No Ct
Wisc Neg 22	Swine	MLN	0	0	No Ct	Neg	No Ct
Wisc Neg 16	Swine	small intestine	0	0	No Ct	Neg	No Ct
Wisc Neg 17	Swine	MLN	0	0	No Ct	Neg	No Ct
VT non-PTB 1	Frog	Kidneys	1	1	No Ct	Neg	No Ct
VT non-PTB 2	Frog	small intestine and lung	1	1	No Ct	Neg	No Ct
VT non-PTB 3	Dove	skin	2	2	No Ct	Neg	No Ct
VT non-PTB 4	feline	skin	1	1	No Ct	Neg	No Ct
VT non-PTB 5	feline	skin	1	1	No Ct	Neg	No Ct
VT non-PTB 6	feline	subcutis	0	0	No Ct	Neg	No Ct
VT non-PTB 7	feline	subcutis	0	0	No Ct	Neg	No Ct
VT non-PTB 8	feline	skin	0	0	No Ct	Neg	No Ct
VT non-PTB 9	feline	skin	0	0	No Ct	Neg	No Ct
VT non-PTB 10	feline	skin	1	1	No Ct	Neg	No Ct
VT non-PTB 11	canine	skin	0	0	No Ct	Neg	No Ct
VT non-PTB 12	Turtle	Lung & Trachea	1	N/A	No Ct	Neg	N/A
VT non-PTB 13	Turtle	Lung & liver	2	N/A	No Ct	Neg	N/A

MLN = mesenteric lymph node, si = small intestine, Neg = Negative, interp. = interpretation, qPC1 = BioRad iCycler MAP<sub>hspX</sub> results, qPCR2 = Stratagene Mx3005p MAP hspX results, AFS = Acid Fast Score

**Table 2.2:** Fecal MAP culture positive Johne's cases

Fecal MAP culture positive cases, species, tissue, Acid Fast Score (AFS), quantitative polymerase chain reaction results (qPCR), interpretation of iCycler MAP hspX qPCR assay defined by IS900 qPCR assay results (interp.), and acid fast bacteria area index (AFBAI)									
Block ID#	Species	Tissues	AFS (0-4) Pathologist 1	AFS (0-4) Pathologist 2	MAP hspX qPCR 1	interp.	MAP hspX qPCR 2	IS900 qPCR	AFBAI (µm <sup>2</sup> )
Wisc 1	Bovine	Small Intestine	1	1	44.3	Negative	39.8	No Ct	N/A
Wisc 2	Bovine	MLN	1	1	36.5	Pos	36.4	32.4	N/A
Wisc 3	Bovine	Small Intestine	3	3	33.1	Pos	32.7	31.8	N/A
Wisc 4	Bovine	MLN	2	2	31.8	Pos	31.5	33.1	N/A
Wisc 5	Bovine	small intestine & MLN	4	4	30.3	Pos	30.1	26.7	N/A
Wisc 7	Bovine	Small Intestine	3	3	31	Pos	30.7	29	N/A
Wisc 8	Bovine	Small Intestine	1	1	39.3	Negative	39.6	No Ct	N/A
Wisc 10	Caprine	Small Intestine	4	4	29	Pos	29.2	36.3	N/A
Wisc 11	Caprine	Small Intestine	4	4	28.8	Pos	28.5	23.8	N/A
Wisc 19	Bovine	Small Intestine	2	3	31.2	Pos	30.9	21.3	N/A
Wisc 23	Bovine	Small Intestine	2	2	33.2	Pos	32.9	33.6	N/A
Wisc 25	Bovine	Small Intestine	4	4	25.7	Pos	25.7	38.3	N/A
Wisc 26	Caprine	MLN	4	4	29.7	Pos	29.7	37.2	N/A
Wisc 31	Bovine	Small Intestine	0	0	No Ct	Negative	40.5	No Ct	N/A
Wisc 32	Caprine	Small Intestine	4	4	26.2	Pos	26.1	40	N/A
OKST 1	Bovine	small intestine	4	4	33.8	Pos	33.8	28.9	651613
OKST 2	Bovine	small intestine	3	3	No Ct	Negative	44.8	No Ct	105334
OKST 4	Bovine	small intestine	0	0	36.2	Pos	35.9	34.9	70826
OKST 5	Bovine	small intestine	4	4	20.4	Pos	21.7	17.9	38273642
OKST 6	Ovine	small intestine	4	4	23.7	Pos	26.0	12.9	70328554
OKST 8	Ovine	small intestine & MLN	4	4	23.2	Pos	25.6	20.3	24043482
OKST 9	Bovine	small intestine	4	4	21.2	Pos	22.4	17.2	35537073
OKST 10	Bovine	small intestine	4	4	19.5	Pos	21.6	16.7	91124216
OKST 11	Bovine	small intestine	1	1	35.7	Pos	38.4	13.4	44394
OKST 12	Bovine	small intestine	0	0	39.6	FN	35.3	27.8	18927
OKST 13	Bovine	small intestine	0	0	38.9	FN	38.2	26.1	36551
OKST 15	Bovine	small intestine & MLN	3	3	33.9	Pos	34.8	31.1	645427
UC Davis 2	Bovine	small intestine	2	2	29.6	Pos	30.9	29.3	1001070

MLN = mesenteric lymph node, si = small intestine, FN = False Negative, Pos = Positive, qPCR1 = BioRad iCycler MAP hspX results, qPCR2 = Stratagene MX3005p MAP hspX results

**Table 2.3: Additional Johne's disease cases**

Additional Johne's disease cases (fecal MAP culture data negative or unavailable), species, tissue, Acid Fast Score (AFS), quantitative polymerase chain reaction results (qPCR), interpretation of iCycler MAP hspX qPCR assay defined by IS900 qPCR assay results (interp.), and acid fast bacteria area index (AFBAI)											
BlockID#	Species	Tissues	AFS (0-4)		MAP hspX		MAP hspX		Additional tests	IS900 qPCR	AFBAI (µm <sup>2</sup> )
			Pathologist 1	Pathologist 2	qPCR 1	interp.	qPCR 2				
VT 1	Caprine	small intestine	2	2	36.4	Pos	32.1	N/A		34.5	551239
VT 3	Caprine	MLN & small intestine	0	0	31.9	Pos	34.9	N/A		26.6	1175181
VT 4	Caprine	small intestine	3	3	34.4	Pos	36.6	N/A		38.8	604562
VT 5	Caprine	small intestine	2	2	32.6	Pos	35.5	N/A		29.6	1653237
VT 8	Bovine	colon	3	3	40.4	FN	33.2	N/A		34.6	564504
VT 9	Bovine	colon & small intestine	3	3	31.6	Pos	33.1	N/A		36.1	1296755
VT 12	Bovine	MLN & small intestine	2	2	29.6	Pos	27.2	N/A		24.9	1841447
VT 13	Bovine	small intestine	3	3	30.1	Pos	30.4	N/A		27.6	1759894
VT 14	Bovine	small intestine	3	3	31.6	Pos	33.9	N/A		28.2	1458026
VT 22	Bovine	MLN & small intestine	3	3	35.2	Pos	31.8	N/A		30.6	655054
VT 29	Bovine	colon & small intestine	4	4	26.2	Pos	35.8	N/A		23.3	11812821
VT 30	Bovine	reticulum & MLN	3	3	28.1	Pos	39.5	N/A		24.7	12856575
VT 34	Caprine	small intestine	4	4	28.1	Pos	41.1	N/A		27.7	11798760
VT 37	Caprine	colon & small intestine	4	4	27	Pos	38.0	N/A		24	12878708
LSU 1	Caprine	small intestine	3	3	28.3	Pos	27.6	fMAP culture -		25.1	2705246
LSU 2	Bovine	small intestine	3	3	29.4	Pos	29.4	N/A		26.4	2407712
LSU 3	Bovine	small intestine	4	4	26.2	Pos	27.9	N/A		27.8	6001494
LSU 4	Bovine	small intestine	4	4	27.1	Pos	25.9	N/A		27.9	5273268
LSU 5	Bovine	MLN & small intestine	1	1	34	Pos	34.8	N/A		31.6	648982
LSU 6	Caprine	small intestine	4	4	26.9	Pos	27.6	N/A		24.7	12827781
LSU 7	Bovine	MLN & small intestine	4	4	26.1	Pos	27.6	N/A		23.7	12996696
LSU 8	Bovine	small intestine	3	3	29.1	Pos	35.9	N/A		26.9	3085876
LSU 9	Bovine	small intestine	4	4	25.1	Pos	37.4	N/A		22	12509983
LSU 10	Bovine	small intestine	3	3	33	Pos	No Ct	N/A		28.1	753687
LSU 11	Bovine	MLN & small intestine	4	4	24.6	Pos	26.4	N/A		23.8	13715015
LSU 12	Bovine	small intestine	3	4	25.2	Pos	27.0	sELISA +, fMAP PCR +		23.8	12176924
LSU 13	Caprine	colon & small intestine	3	3	27.9	Pos	33.5	sELISA +, fMAP PCR +		25.8	5944172
LSU 14	Bovine	small intestine	4	4	26.5	Pos	29.7	N/A		23.5	12259195
LSU 15	Bovine	small intestine	2	2	34	Pos	32.5	fMAP culture -		32.9	1320622
Corn 1	Bovine	small intestine	4	4	35.9	Pos	35.1	N/A		21	3617
Corn 2	Bovine	MLN	2	3	31.68	Pos	30.2	N/A		25.2	9798926
Corn 3	Caprine	small intestine	4	4	34.75	Pos	35.1	N/A		31.6	489277
Corn 4	Bovine	small intestine	4	4	31.11	Pos	31.6	N/A		24.6	42774
Corn 5	Caprine	small intestine	4	4	34.91	Pos	41.6	N/A		23.7	320582
Corn 6	Bovine	small intestine	2	2	35.83	Pos	36.2	N/A		26.3	26242
Corn 7	Bovine	small intestine	4	4	28.67	Pos	25.6	N/A		30.6	5153619
Corn 8	Caprine	small intestine	3	3	30.95	Pos	33.2	N/A		30.7	8983872
Corn 9	Bovine	small intestine	4	4	36.5	Pos	36.7	N/A		33.8	56070
Corn 10	Bovine	small intestine	4	4	35.07	Pos	35.5	N/A		30.6	68708
WSU 1	Bovine	small intestine	1	1	34.52	Pos	34.6	N/A		25.3	743760
WSU 2	Bovine	small intestine	4	4	37.49	Pos	39.0	N/A		36.2	291645
WSU 3	Ovine	small intestine	4	4	35.17	Pos	34.9	N/A		36	614787
WSU 4	Ovine	MLN & small intestine	4	4	No Ct	FN	37.2	N/A		28.3	83368
WSU 5	Ovine	small intestine	4	4	35.3	Pos	32.6	N/A		33.4	191010
UC Davis 1	Caprine	small intestine	1	1	36.9	Pos	37.4	sAGID +		33.1	66469
UC Davis 3	Caprine	small intestine	3	3	28.2	Pos	33.8	sELISA +		24.6	3792546
UC Davis 4	Bovine	small intestine	3	4	29.2	Pos	34.3	N/A		24	10317520
UC Davis 5	Caprine	small intestine	4	4	23.6	Pos	26.2	N/A		20.4	16969164
UC Davis 6	Ovine	small intestine	4	4	20.7	Pos	24.8	N/A		18.3	55314152
UC Davis 7	Ovine	small intestine	4	4	No Ct	FN	25.5	N/A		28.2	54281
UC Davis 8	Ovine	small intestine	3	3	33.4	Pos	30.6	N/A		23.6	718575
UC Davis 9	Ovine	small intestine	4	4	23.3	Pos	22.9	N/A		19.4	31356354
UC Davis 10	Bovine	small intestine	4	4	22.9	Pos	26.9	N/A		38.4	12897019
UC Davis 11	Bovine	small intestine	3	3	25.7	Pos	27.3	N/A		28	1886536
UC Davis 12	Caprine	small intestine	2	2	30.6	Pos	No Ct	sELISA +, fMAP PCR+		28.8	8713335
UC Davis 13	Caprine	small intestine	4	4	27.5	Pos	No Ct	sELISA +		25	6320555
UC Davis 14	Bovine	small intestine	0	0	35.2	Pos	37.9	siMAP PCR+, sELISA -		13.9	153278

MLN = mesenteric lymph node, si = small intestine, FN = False Negative, Pos = Positive, qPCR1 = BioRad iCycler MAP hspX results, qPCR2 = Stratagene MX3005p MAP hspX results, sAGID+ = serum MAP agarose gel immunodiffusion positive, sELISA+ = serum MAP ELISA positive, fMAP PCR+ = fecal MAP PCR positive, siMAP PCR+ = small intestine tissue MAP PCR positive, fMAP culture - = fecal MAP culture negative

**Table 2.4:** Comparisons of MAP *hspX* qPCR result with different assays

		Adiagene ® AdiaVet IS900 based qPCR assay				Adiagene ® AdiaVet IS900 based qPCR assay from positive fecal MAP culture cases			
		N = 85	Postive	Negative			N = 28	Postive	Negative
Tetracore® VetAlert MAP <i>hspX</i> based qPCR assay	Positive		76	0	Tetracore® VetAlert MAP <i>hspX</i> based qPCR assay	Positive		22	0
	Negative		5	4		Negative		2	4
		Visible AF Bacteria present in samples				Adiagene ® AdiaVet IS900 based qPCR assay & visible AF Bacteria present in samples			
		N = 85	Postive	Negative			N = 79	Postive	Negative
Tetracore® VetAlert MAP <i>hspX</i> based qPCR assay	Positive		73	3	Tetracore® VetAlert MAP <i>hspX</i> based qPCR assay	Positive		73	0
	Negative		6	3		Negative		3	3

## References

- 1 Alexander KA, Pleydell E, Williams MC, Lane EP, Nyange JF, Michel AL: Mycobacterium tuberculosis: an emerging disease of free-ranging wildlife. *Emerg Infect Dis* **8**: 598-601, 2002
- 2 Buergelt CD, Hall C, McEntee K, Duncan JR: Pathological evaluation of paratuberculosis in naturally infected cattle. *Vet Pathol* **15**: 196-207, 1978
- 3 Collins MT, Gardner IA, Garry FB, Roussel AJ, Wells SJ: Consensus recommendations on diagnostic testing for the detection of paratuberculosis in cattle in the United States. *J Am Vet Med Assoc* **229**: 1912-1919, 2006
- 4 Corpa JM, Garrido J, Garcia Marin JF, Perez V: Classification of lesions observed in natural cases of paratuberculosis in goats. *J Comp Pathol* **122**: 255-265, 2000
- 5 Dedhia P, Tarale S, Dhongde G, Khadapkar R, Das B: Evaluation of DNA extraction methods and real time PCR optimization on formalin-fixed paraffin-embedded tissues. *Asian Pac J Cancer Prev* **8**: 55-59, 2007
- 6 Ellingson JL, Bolin CA, Stabel JR: Identification of a gene unique to Mycobacterium avium subspecies paratuberculosis and application to diagnosis of paratuberculosis. *Mol Cell Probes* **12**: 133-142, 1998
- 7 Gonzalez J, Geijo MV, Garcia-Pariente C, Verna A, Corpa JM, Reyes LE, Ferreras MC, Juste RA, Garcia Marin JF, Perez V: Histopathological classification of lesions associated with natural paratuberculosis infection in cattle. *J Comp Pathol* **133**: 184-196, 2005
- 8 Hunnam JC, Wilson PR, Heuer C, Mackintosh CG, West DM, Clark RG: Histopathology of Grossly Normal Mesenteric Lymph Nodes of New Zealand Farmed Red Deer (*Cervus elaphus*) Including Identification of Lipopigment. *Vet Pathol*, 2010

- 9 Johnson-Ifearegulu Y, Kaneene JB, Lloyd JW: Herd-level economic analysis of the impact of paratuberculosis on dairy herds. *J Am Vet Med Assoc* **214**: 822-825, 1999
- 10 Ott SL, Wells SJ, Wagner BA: Herd-level economic losses associated with Johne's disease on US dairy operations. *Prev Vet Med* **40**: 179-192, 1999
- 11 Perez V, Garcia Marin JF, Badiola JJ: Description and classification of different types of lesion associated with natural paratuberculosis infection in sheep. *J Comp Pathol* **114**: 107-122, 1996
- 12 Plante Y, Remenda BW, Chelack BJ, Haines DM: Detection of *Mycobacterium* paratuberculosis in formalin-fixed paraffin-embedded tissues by the polymerase chain reaction. *Can J Vet Res* **60**: 115-120, 1996
- 13 Ravva SV, Stanker LH: Real-time quantitative PCR detection of *Mycobacterium avium* subsp. paratuberculosis and differentiation from other mycobacteria using SYBR Green and TaqMan assays. *J Microbiol Methods* **63**: 305-317, 2005
- 14 Shi SR, Cote RJ, Wu L, Liu C, Datar R, Shi Y, Liu D, Lim H, Taylor CR: DNA extraction from archival formalin-fixed, paraffin-embedded tissue sections based on the antigen retrieval principle: heating under the influence of pH. *J Histochem Cytochem* **50**: 1005-1011, 2002
- 15 Taddei R, Barbieri I, Pacciarini ML, Fallacara F, Belletti GL, Arrigoni N: *Mycobacterium* porcinum strains isolated from bovine bulk milk: implications for *Mycobacterium avium* subsp. paratuberculosis detection by PCR and culture. *Vet Microbiol* **130**: 338-347, 2008
- 16 Tavoranpanich S, Gardner IA, Anderson RJ, Shin S, Whitlock RH, Fyock T, Adaska JM, Walker RL, Hietala SK: Evaluation of microbial culture of pooled fecal samples for

- detection of *Mycobacterium avium* subsp *paratuberculosis* in large dairy herds. *Am J Vet Res* **65**: 1061-1070, 2004
- 17 Valentin-Weigand P, Goethe R: Pathogenesis of *Mycobacterium avium* subspecies *paratuberculosis* infections in ruminants: still more questions than answers. *Microbes Infect* **1**: 1121-1127, 1999
  - 18 Vary PH, Andersen PR, Green E, Hermon-Taylor J, McFadden JJ: Use of highly specific DNA probes and the polymerase chain reaction to detect *Mycobacterium paratuberculosis* in Johne's disease. *J Clin Microbiol* **28**: 933-937, 1990
  - 19 Whittington RJ, Reddacliff L, Marsh I, Saunders V: Detection of *Mycobacterium avium* subsp *paratuberculosis* in formalin-fixed paraffin-embedded intestinal tissue by IS900 polymerase chain reaction. *Aust Vet J* **77**: 392-397, 1999
  - 20 Zsikla V, Baumann M, Cathomas G: Effect of buffered formalin on amplification of DNA from paraffin wax embedded small biopsies using real-time PCR. *J Clin Pathol* **57**: 654-656, 2004

## Correlation of Quantitative Histopathology with Quantitative Polymerase Chain Reaction in the Diagnosis of Johne's disease

### ABSTRACT

Gross and microscopic lesions in Johne's disease vary according to clinical stage. To examine the correlation of *Mycobacterium avium* subspecies *paratuberculosis* (MAP) specific quantitative polymerase chain reaction (qPCR) results with acid fast quantitative histopathology, eighty-five formalin-fixed paraffin-embedded (FFPE) tissue blocks from 70 ruminants (8 ovine, 17 caprine, & 45 bovine) diagnosed with Johne's disease by necropsy and histopathology were examined by quantitative histopathology and assessed for bacterial load by qPCR.

Sections of FFPE tissues contained either mesenteric lymph nodes or intestine with granulomatous inflammation and varying numbers of acid fast bacteria. Ziehl-Neelsen-stained slides were scored (0-4) based on the numbers of acid fast bacteria (AFB). Additionally an acid fast bacteria index (AFAI) (acid-fast bacteria area percentage in twenty-five 20x magnified fields multiplied by the total tissue area) was calculated on a subset of the samples (n = 70) using a Leica inverted digital imaging microscope DMI6000B and Lab View morphometric software.

In comparing the MAP *hspX* qPCR cycle threshold results (Ct) to the quantitative histopathology, the mean Ct decreased as the acid fast score (AFS) increased. There was medium-strong rank correlation between of the AFS and iCycler MAP *hspX* qPCR Ct values (Spearman's  $\rho = -0.5371$ , n = 85,  $p < 0.0001$ ). There was a strong negative linear correlation (Pearson's  $r = < -0.6562$ ,  $p < 0.001$ , n = 70) between the acid-fast bacteria area index (AFBAI) and the iCycler MAP *hspX* qPCR Ct results. Further, the correlation of results was strongest at lower Ct values and higher AFBI, whereas the correlation of the results was weaker at higher Ct values and lower AFBI.

This study confirms that when using the freeze/boil extraction method on FFPE tissues the MAP specific *hspX* & IS900 qPCR results correlate with the quantitative histopathology of the corresponding slides supporting the use of this technique for evaluating the severity of infection.

## Introduction

*Mycobacterium avium* subspecies *paratuberculosis* (MAP) causes Johne's disease (JD) a chronic wasting disease of ruminants. MAP is the slowest growing of all cultivatable mycobacteria,<sup>19</sup> making culture a cumbersome method of paratuberculosis diagnosis. Primary culture isolation of MAP from veterinary clinical samples can take as long as 24 weeks.<sup>27</sup>

The most common route of infection is through oral ingestion of MAP as fecal, milk or colostrum contaminants. While transmission is generally by the fecal oral route<sup>15</sup>, in utero transmission has also been reported in sheep, goats and cattle.<sup>18,31,40</sup> While usually infected in the first months of life, the majority of ruminants do not progress to clinical disease (emaciation, diarrhea in some species) for several years.<sup>36</sup>

It is believed that most animals are able to control MAP infections as most ruminants experimentally infected with MAP fail to develop lesions.<sup>30,33</sup> While diarrhea is a prominent clinical sign in cattle, it only rarely develops in the latest stages of JD in sheep and goats.<sup>3,20,31</sup>

Based on growth characteristics and host preferences two major strains have been described. Historically these strains were named based on the species which they were first isolated from (sheep (S-type) and cow (C-type)), although the C-type strains could be cultured from sheep and vice versa. To avoid confusion these strains were renamed type I for (S-type) and type II for C-type MAP.<sup>32</sup> Based on genetic assays, a new intermediate, designated type III was described.<sup>5</sup> However, recent genomic comparisons support the strain divisions into just two strain types (type S and C) with the intermediate (type III) strain listed under the S-type strain.<sup>1</sup> In general, genetic MAP strain diversity is limited, especially under type C MAP strains.<sup>22</sup>

Differences in strain type and immunopathology in JD have been described. S-type strains are reported to be more likely to up-regulate pro-inflammatory cytokines associated with

protective immunity and fewer acid fast bacteria in lesions (paucibacillary form).<sup>17,21</sup> Conversely, C-type strains have been reported not to induce protective immunity and when isolated from ovine paratuberculosis cases, Langhans multinucleate giant cells are a common feature in the granulomatous inflammation.<sup>17,21,38</sup>

A highly diagnostic gross lesion in clinically ill ruminants in late stages of Johne's disease is segmental distal small intestine thickening with a corrugated mucosal surface.<sup>2,7,24</sup> The microscopic intestinal lesions are characterized by focal, multifocal, or diffuse mucosal infiltration of macrophages and multinucleate giant cells that may contain few (paucibacillary) or myriad (multibacillary) acid-fast rods.<sup>2,7,12,24</sup> The adjacent lymphoid tissue (Peyer's patches) and mesenteric lymph node chain may be infiltrated by similar inflammatory cells with intracellular MAP.<sup>2,7,24</sup> In earlier stages of infection, gross lesions may be absent and acid-fast organisms may be so few as to be undetectable.<sup>12</sup>

Quantitative histopathology is the quantification of specific identifiable microscopic changes or lesions. In diagnostic pathology, the mitotic index is one of the more commonly employed measures in neoplastic lesions and is applied to assess the biologic behavior of such neoplastic conditions. Quantitative measures applied in infectious disease lesions include enumeration of inclusion bodies, microorganisms, or degenerative changes and can be used to aid in the prognosis, to help direct therapy, or to investigate clinical responses, pathogenesis and immunology.<sup>11,13,14,23,35</sup> Quantitative histopathology has been used in sheep with Johne's disease to describe differences in microscopic lesions with lesions that have 10 or fewer acid fast bacteria (AFB) per macrophage as paucibacillary lesions, and lesions with >10 AFB per macrophage as multibacillary lesions.<sup>4</sup> Quantitative histopathology has also been applied to describe the lesion differences in goats reflective of the immunopathologic response where

“tuberculoid” responses contain few AFB, lepromatous responses contain many AFB and borderline responses are described as being between these two polar responses.<sup>7,30</sup>

Real-time quantitative polymerase chain reaction (qPCR) assays use one or more specific DNA targets and the PCR technique to simultaneously amplify and quantitate the DNA amplicons. This technique can be applied to formalin-fixed paraffin-embedded (FFPE) tissues to identify and quantify specific pathogens (e.g. viruses, bacteria, fungi). Microscopic lesions and visible quantification of intra-lesional microorganisms (quantitative histopathology) in theory should correlate with qPCR assay results specific for the microorganism in FFPE tissues. An evaluation of qPCR applied on FFPE tissues infected with *Chlamydia pneumoniae* showed a negative correlation of the cycle threshold (Ct) to the number of inclusions detected by immunohistochemical histopathology.<sup>23</sup> Another study comparing *Mycobacterium tuberculosis* qPCR results from FFPE tissues with the corresponding quantitative acid-fast histopathology concluded that the number of DNA templates detected (number of bacteria) did not correlate and was much higher compared to the quantitative acid fast histopathology.<sup>11</sup> Tuberculosis is generally considered a paucibacillary disease and few acid fast bacteria are detected in tissue sections compared to Johne’s disease. MAP specific conventional IS900 PCR has been applied to FFPE tissues and reported that the DNA product band intensities correlated with quantitative acid fast histopathology.<sup>39</sup> No reports have documented MAP specific qPCR results applied to FFPE tissues with a correlation of microscopic lesions.

The development of PCR assays for the detection of MAP-specific genetic sequences such as the insertion sequence 900 (IS900)<sup>26,37</sup> and MAP *hspX*<sup>9</sup> has expanded the repertoire of diagnostic targets for Johne’s disease testing. Direct fecal PCR is now an accepted diagnostic assay for the National Voluntary Bovine Johne’s Disease Control Program in the United States.<sup>6</sup>

Conventional PCR has limited sensitivity because a certain amount of starting DNA must be present in the sample used in the PCR to produce a visible band (DNA amplicon product). This is more often a problem with PCR applied to clinical samples (tissues) than from culture samples of MAP. Additionally, in conventional PCR testing, the intensity of the bands (DNA product from the PCR) can give a rough quantification of the original amount of infectious agent.

Conversely, quantitative real-time PCR is more sensitive than conventional PCR because the detection of the fluorescent signal by the machine is more sensitive than visualization of a PCR band. Additionally, the detection of the fluorescent signal occurs during the reaction (real-time), whereas in conventional PCR the visualization of the product (amplicon) band occurs after the reaction is complete, when the product (amplicon) is separated based on size by the net-negative charge of the sugar-phosphate backbone of the amplicon. According to one paratuberculosis commercial qPCR kit manufacturer<sup>a</sup>, their paratuberculosis assay is sensitive enough to detect as few as a single DNA template and would give a Ct value of 38 on the BioRad iCycler thermocycler. Finally, the quantification of DNA product during real-time PCR is more precise than quantification based on the intensity of the DNA product band.

There are 15-20 reported copies of the IS900 genes<sup>16,28</sup> compared to only 1 copy of the *hspX* gene<sup>9,10</sup> in the MAP genome. Theoretically, this would suggest that the IS900 gene target would be more sensitive for detection, but the *hspX* target would be more precise in the quantification.

Recently commercial real-time PCR assays have been developed that target MAP specific *hspX* and IS900 genes. These assays are now commonly used to detect MAP in bovine fecal samples. These assays take less time than conventional PCR, because gel electrophoresis is

not required and results are based on cycle threshold (Ct) values provided by a real-time PCR thermocycler.

We predicted that a simple freeze/boil DNA extraction technique could be used on FFPE tissues and the extract tested by a commercial MAP *hspX* based qPCR assay. We hypothesized that the qPCR results would correlate with the quantitative histopathology of slides prepared from respective FFPE tissue blocks. We expect this new qPCR technique combined with quantitative histopathology would prove useful when applied in research and clinical studies to evaluate similarities and differences in Johne's disease by several variables (e.g., species, geographical, strain, clinical responses to treatment, etc.).

## **Materials and Methods**

FFPE tissue blocks from animals diagnosed with Johne's disease were collected from several veterinary diagnostic laboratories. Each animal representing a Johne's disease case was a clinically ill (emaciated) adult from a herd with prior cases of Johne's disease, was fecal culture positive for MAP (n=28), and had gross and histopathologic lesions of Johne's disease (granulomatous infiltrate with intracellular acid fast organisms) according to the laboratory contributing the tissue block.

### Acid Fast Score (AFS):

The first portion of this study entailed two pathologists independently examining and assigning an acid-fast score to sections from the FFPE tissue blocks. The FFPE tissue blocks had been prepared by standard protocols (fixed in buffered formalin, processed with xylene and alcohol and embedded in paraffin) and were coded to conceal whether they were positive or negative samples. Each block contained at least one tissue relevant for Johne's disease diagnosis

(ileum or mesenteric lymph node). A 5  $\mu\text{m}$  section was sliced by microtome from each tissue block, fixed on a glass slide and stained with hematoxylin and eosin (H&E) for microscopic assessment of granulomatous inflammation. Granulomatous inflammation consistent with Johne's disease was seen on all slides prepared from these blocks according to both pathologists. Another section was stained with Ziehl-Neelsen's stain and scored for the quantity of acid-fast bacteria (AFB) in the tissue sections where 0 = none, 1 = rare/scant macrophages containing few AFB, 2 = occasional clusters of macrophages containing clusters of AFB, 3 = moderate numbers macrophages filled with AFB, 4 = numerous macrophages packed with AFB (**Figure 3.1**).

#### Acid Fast Bacteria Area Index (AFBAI):

A subset of 70 Ziehl-Neelsen's stained slides from the 85 Johne's disease cases were scanned and imaged with a Leica DMI3000B inverted digital microscope.<sup>g</sup> In this process, a  $5.7 \times 10^8 \mu\text{m}^2$  to  $1.3 \times 10^9 \mu\text{m}^2$  area of the slide was scanned using the 5x objective and used to calculate the total tissue area (TTA). A Leica digital DFC340Fx digital camera was used to image the slides using a bright-field and fluorescent channel. The bright field channel images were set a 4 milliseconds exposure time, a gain of 1, and intensity of 10. The fluorescent channel settings used 400 milliseconds exposure, gain of 2, and intensity of 5. Using Lab-View morphometric software<sup>h</sup>, the bright-field and fluorescent images were overlapped and used to calculate the total tissue area (**Figure 3.2**).

Next, the Leica D490A color digital camera was used with the 20x objective to scan a 5 x 5 grid (25 images,  $9 \times 10^6 \mu\text{m}^2$  area) with the tiling microscope in a region where AFB are typically found, e.g. mucosa or lymph node sinus (**Figure 3.3**). Utilizing both a bright field (visible light) camera, and a fluorescent camera and light source, the bright field images were processed for specific red color shifts, consistent with the Acid Fast Bacteria (AFB). The regions

of interest highlighted by this method were then overlaid onto the fluorescent images of fluorescing tissue. Highlighted areas without tissue fluorescence were mostly caused by extraneous matter on the slides and were excluded. Highlighted areas with tissue fluorescence were consistently found to coincide with AFB, and their pixel areas were recorded. This double filter method allowed the program to eliminate common sources of error, such as smooth muscle or extraneous matter. The bright-field settings were a 20 milliseconds exposure time, gain set a 1, color saturation was 100 and intensity was 85-100. The fluorescent channel settings used a DFT filter, exposure time of 1 second, gain of 2, color saturation of 100, and intensity of 5. After capturing the image data, the images were analyzed using the LabView® morphometric software<sup>h</sup> and the total area of AFB in the  $9 \times 10^6 \mu\text{m}^2$  area was calculated. Images were analyzed to detect color pixels of red to pink that were specific for acid-fast bacteria and eliminate red pixels that were of non-specific staining. This protocol was established by trial and error after testing several slides in the detection of acid-fast bacteria.

Once the AFB pixel area was determined, it was possible to determine the % of overall AFB pixels to overall tissue pixels, as found by the fluorescence images. The bright field images and the fluorescent images were tiled into an image mosaic for visual comparison of the results.

Finally, using the data (AFB area in a 5 x 5 grid imaged using a 20x objective & TTA imaged using a 5x objective) obtained from the tiling digital microscope a acid fast bacteria index (AFBAI) was calculated where the TTA was multiplied by the area of acid fast bacteria obtained from the 20x images. This AFBAI value was used to compare the quantitative histopathology results to the quantitative PCR results to determine correlation.

### MAP Quantitative PCR (qPCR) testing:

For MAP qPCR testing, 25 µm scrolls were cut by microtome from each of the FFPE tissue blocks. To prevent cross-contamination, the microtome blade and forceps were immersed and wiped clean with a 10% bleach (sodium hypochlorite) solution between each block. To screen for the contamination, negative sample's scrolls were cut after the positive sample's scrolls were cut. MAP DNA was extracted by the boil-freeze method as described previously.<sup>39</sup> Briefly, scrolls were transferred to sterile 1.5 ml screw-cap graduated conical tubes<sup>e</sup> and centrifuged for 1 minute at 24,000 x g. To each of the pelleted tissue scrolls 200 µl of 0.5% Tween 20 was added and the sample tubes were placed in a heat block at 100°C for 10 minutes. The tubes were then immersed in liquid nitrogen for 15-20 seconds to snap-freeze the contents. The boil/snap-freeze steps were repeated twice followed by an additional boil step. The tubes were then centrifuged for 20 minutes at 850 x g. After centrifugation, the resultant liquid was transferred to coded sterile 1.5ml microcentrifuge tube<sup>d</sup> and frozen at -20°C for storage.

The second section of the study entailed testing the extracted DNA for MAP *hspX* according to the PCR manufacturer's instructions.<sup>a</sup> All DNA extracts were run on a BioRad iCycler<sup>b</sup> with a positive result defined as  $Ct \leq 38$  (the cut-off established by the manufacturer based on validation with bovine fecal samples). For samples that did not register a Ct value (No Ct), a Ct value of 45 (the total number of cycles by the thermocycler) was assigned for statistical comparisons. Additionally, the DNA extracts from the FFPE tissue blocks of the 85 Johnne's disease cases were also tested using the commercial IS900 based qPCR assay<sup>i</sup> using the BioRad iCycler<sup>b</sup> thermocycler and results were recorded as positive if the qPCR Ct result was  $< 45$  for the FAM-490 fluorescent dye as per the manufacturer's interpretation instructions.

The final section of study entailed correlating the results of the MAP *hspX* and IS900 qPCR with the AFS or AFBAI. JMP 9.0 statistical software was used for the statistical comparisons.

## Results

There was excellent agreement between the two pathologists' acid-fast-scores ( $k = 0.931$ ,  $n = 85$ ) on slides from the 85 FFPE tissue blocks from 70 ruminants diagnosed with Johne's disease.

Of the 85 FFPE tissue blocks examined, forty were given an AFS of 4, twenty-one received an AFS of 3, eleven received an AFS of 2, seven received an AFS of 1 and six received an AFS of 0. With these results, 61 were given an acid fast score  $>2$ , whereas 24 were scored 2 or lower. Defining multibacillary lesions as an AF score of  $>2$ , these results suggest that lesions from animals diagnosed with Johne's disease at necropsy tend to be almost two times more likely to be multibacillary lesions.

There was an inverse rank correlation between the AFS and the MAP *hspX* qPCR Ct results. That is as the AFS increased, the Ct results decreased (Spearman's  $\rho = -0.5371$ ,  $n = 85$ ,  $p < 0.0001$ ) (**Figure 3.4**). Regression analysis showed that a unit increase in AFS was associated with a 2.38 decrease in Ct value ( $Y = -2.38 + 38.52$ ,  $p < 0.05$ ). Similarly there was an inverse rank correlation between the AFS and MAP IS900 qPCR Ct results (Spearman's  $\rho = -0.2679$ ,  $n = 85$ ,  $p = 0.0132$ ) and regression analysis showed that a unit increase in AFS was associated with a 1.14 decrease in Ct value ( $Y = -1.14X + 31.81$ ,  $p < 0.05$ ).

The iCycler MAP *hspX* PCR assays were positive in 38/40 (95%) of blocks with an acid-fast score of "4", 19/21 (90.5%) scored as "3", 11/11 (100%) scored as "2", 5/7 (71.4%) scored

as a “1” and 3/6 (50.0%) slides with no microscopically visible acid fast rods (score = 0) (**Table 3.1**). MAP qPCR Ct results ranged from 19.5 to 45 Ct times.

Another set of correlation statistics were determined from a subset of samples (n=70) that were imaged with the Leica inverted digital microscope and an acid fast bacteria area index (AFBAI) was computed using LabView<sup>h</sup> software. In this comparison, the AFBAI results were compared to the MAP *hspX* qPCR results and showed a strong negative linear correlation (Pearson's  $r = -0.6562$ ,  $p < 0.0001$ ,  $n = 70$ ) (**Figure 3.5**). The AFBAI results were also compared to the MAP IS900 qPCR results and had a medium-strong negative linear correlation (Pearson's  $r = -0.5529$ ,  $p < 0.0001$ ,  $n = 70$ )

Additionally the iCycler MAP *hspX* qPCR Ct and AFBAI data were divided into two equal segments: qPCR Ct 31.11 to 45 and 19.5 to 30.95 or AFBAI  $3617\mu\text{m}^2$  to  $145802\mu\text{m}^2$  and  $163237\mu\text{m}^2$  to  $91100000\mu\text{m}^2$ . The individual Pearson's correlation coefficients of each segment were then determined and showed the lower segments' correlation coefficients ( $r_2$ ) were repeatedly stronger compared to the upper segments' correlation coefficients ( $r_1$ ) (**Figure 3.7**). This shows stronger linear correlation between AFBAI and qPCR results for tissues with more bacteria.

The bovine FFPE tissue blocks had the lowest average AFS (2.62) and the highest average MAP *hspX* qPCR Ct result (33.0, n=55). Sheep FFPE tissue blocks had the highest average AFS (3.89) and lowest average MAP *hspX* qPCR Ct result (31.6, n = 9). The goat FFPE samples had an average AFS of 2.88 and the second lowest mean MAP *hspX* qPCR Ct result (31.9, n=21). Individually each species showed a statistically significant medium to strong negative linear correlation ( $r -0.6511$  to  $-0.7957$ ) between the AFBAI and BioRad iCycler MAP *hspX* qPCR Ct values (Table 3.2).

## Discussion & Conclusions

The total acid-fast bacteria area of the tissue section would be the ideal value for correlation with the MAP *hspX* qPCR result from the associated FFPE tissue block. Using the Leica digital inverted microscope, each color images used 5 megabytes of data regardless of objective magnification. The 20x objective provides the minimum resolution necessary for precise acid fast bacteria area calculation using the Lab-View morphometric software. However, it would require approximately an 80 x 80 grid (6,400 images) to image an entire slide with the 20x objective and would use approximately 32 gigabytes of data to produce the image. This would be beyond our computer's capabilities (~ 2 gigabyte) for image analysis. To overcome this, an acid fast bacteria area index (AFBAI) was created that would take into account the total tissue area (TTA) combined with a precise measurement of acid fast bacteria area in a representative sample of the tissue. Despite the erroneous assumption that the acid fast bacteria area is the same in all sections of tissue, the AFBAI provides a more precise data point for stronger correlation with the associated MAP *hspX* qPCR results.

In this study, we show that quantitative histopathology results correlate with the MAP specific quantitative PCR results. Further it is suggested that with 61/85 (72%) tissue blocks scored >2, Johne's disease lesions are typically multibacillary at necropsy. There are slight differences between species and number of acid fast bacteria in tissue at necropsy. On average, sheep had the highest number of acid fast bacteria compared to the other species by our methods.

As demonstrated in the results, the correlation of histopathology with MAP specific qPCR is dependent on the numbers of bacteria within the lesions (e.g. the greater the numbers of bacteria in the lesion, the stronger the correlation with quantitative PCR). Extraction of MAP DNA from FFPE tissue sections by the boil-freeze method is rapid, simple and does not require

volatile solvents such as xylene.<sup>25,39</sup> This commercially available qPCR assay targets the MAP *hspX* gene (vs. the MAP IS900 which is potentially less specific given the IS900-like homologues noted in previous reports).<sup>34</sup> To quantify precisely the method's diagnostic specificity, future evaluation of the diagnostic method should include FFPE tissue scrolls from a statistically significant number of known uninfected animals. When fixing tissue for quantitative PCR assay, because  $\beta$ -glycosidic bonds in purine bases are hydrolyzed at pH 4, care should be taken to ensure that formalin is buffered to limit MAP DNA degradation.<sup>8,29,41</sup> Because FFPE tissue blocks are archived for at least several years, the MAP *hspX* PCR supports retrospective studies investigating the severity, extent and distribution of MAP infections over time in different tissues, varied animal species (including humans), and diverse geographic populations.

In conclusion, the qPCR results (IS900 & MAP *hspX*) correlate well with the quantitative histopathology results. With the ease of use of these qPCR protocols, we believe these assays provide additional valuable tools to diagnostic pathology and clinical microbiology research. Clinical studies looking at effects of therapeutics, vaccinations, culling and changes in management could use these qPCR protocols for measuring differences in effect. In the realm of Johne's diagnostics and diagnostic pathology and herd health management this qPCR protocol provides a strong confirmatory test for samples with scant or non-visible acid-fast bacteria by histopathology.

### **Sources and manufacturers**

- a. VetAlert™, Tetracore Inc. Rockville, MD, USA
- b. iCycler, BioRad Laboratories Inc., Hercules, CA, USA
- c. Stratagene Mx3005p, Agilent Technologies Inc., Santa Clara, CA, USA

- d. 1.5 ml microcentrifuge tube, Sigma-Aldrich Inc., St. Louis, MO, USA
- e. 1.5 ml screw top microtube, Sarstedt, Aktiengesellschaft & Co., Germany
- f. JMP® 9.0 Statistical software, SAS Institute Inc., Cary, NC, USA
- g. DMI3000B digital microscope, Leica Microsystems Inc. Buffalo Grove, IL, USA
- h. LabView morphometrical software, National Instruments, Austin, TX, USA
- i. AdiaVet™, Adiagene® Inc., France

## Figures

**Figure 3.1:** Example acid fast scores: Representative acid fast score (AFS) of 1, one macrophage with intracellular acid fast bacteria (AFB) (**arrow**) (**A**), AFS of 2 showing scattered macrophages with scattered macrophages containing intracellular AFB (**B**) AFS of 3 showing moderate numbers of macrophages containing intracellular AFB (**C**) AFS of 4 showing numerous macrophages with intracellular AFB (**D**). All tissues are small intestine stained Ziehl-Neelsen's, 400x magnification.

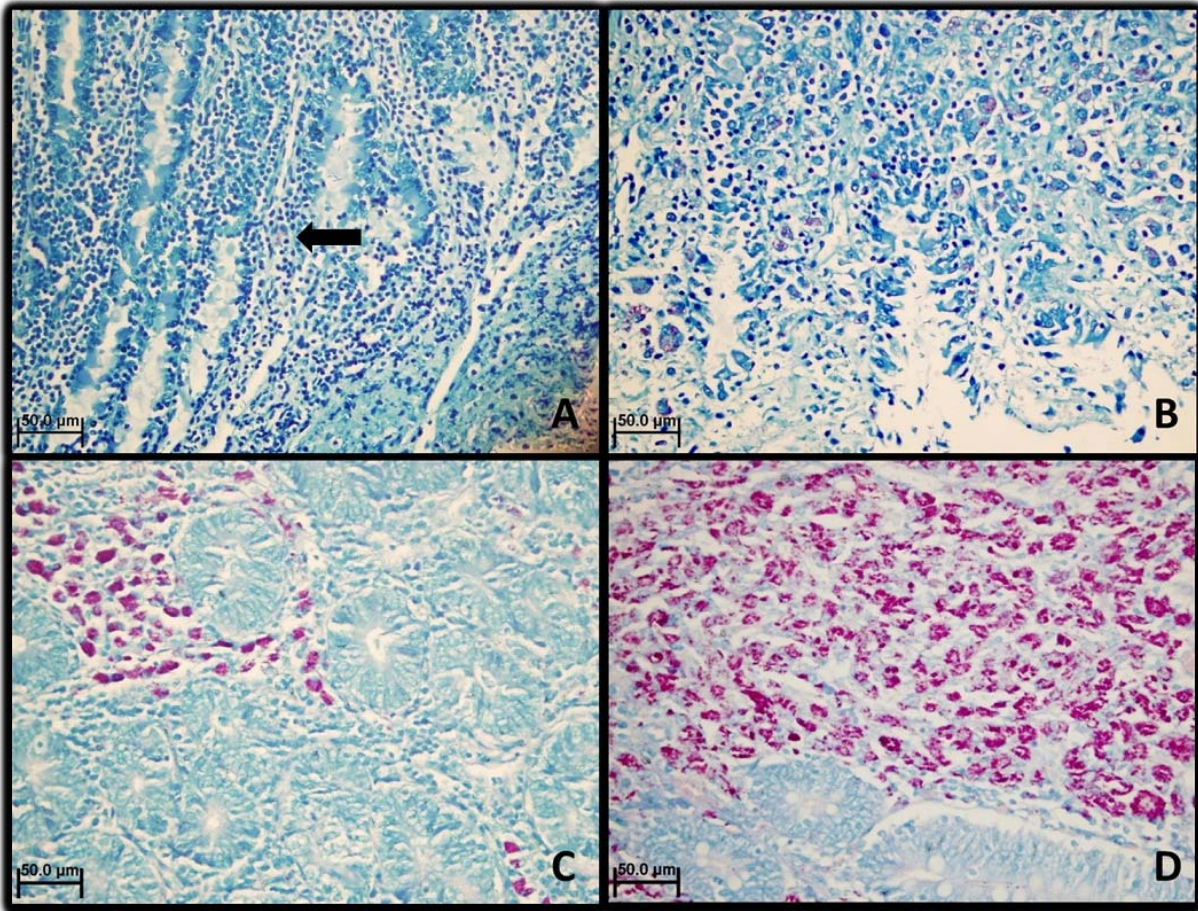


**Figure 3.2:** Example of 5x objective scans of slides used to calculate the total tissue area (TTA): A 7 x 4 grid (28 images) Black & White image (A), 7x4 grid image with florescent camera (B), overlay of black and white and florescent image (C), Identification of total tissue area in pixels identified as blue (D). TTA = sum of all pixels, 1 pixel =  $81\mu\text{m}^2$

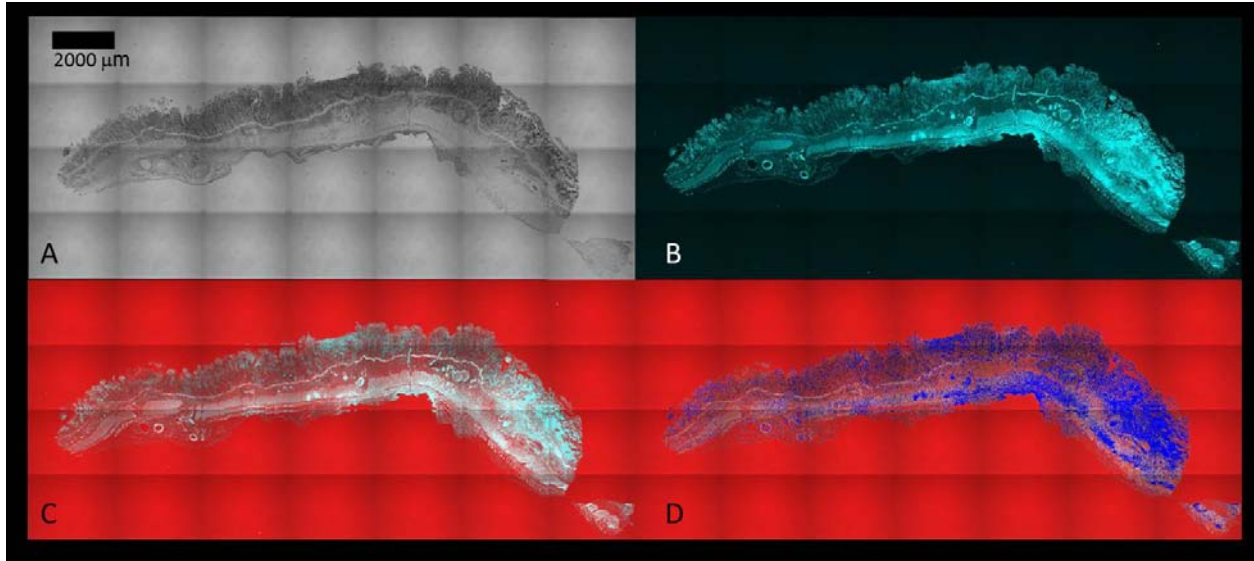


**Figure 3.3:** Examples of a 5 x 5 grid (25 images), 20x objective scan of a slide used to calculate the acid fast bacteria area index (AFBAI) in a section of tissue, Ziehl-Neelsen's stain (**A**), the same 5x5 grid imaged with a fluorescent camera highlighting the acid fast bacteria (**B**), the LabView® morphometric software detection of acid fast bacteria highlighted as green in the same 5x5 grid (**C**).

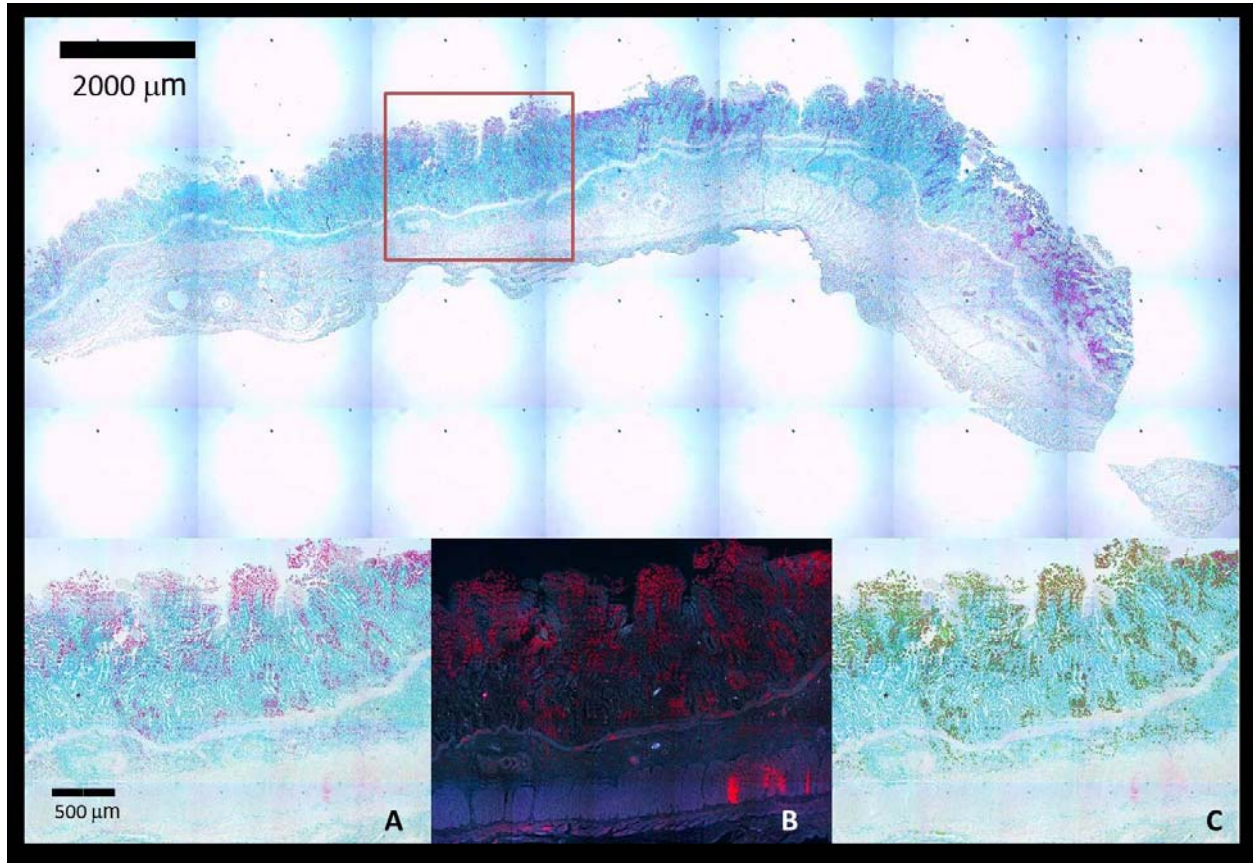


**Figure 3.4:** Rank Correlations between Acid Fast Score (AFS) and MAP qPCR Cycle threshold (Ct)

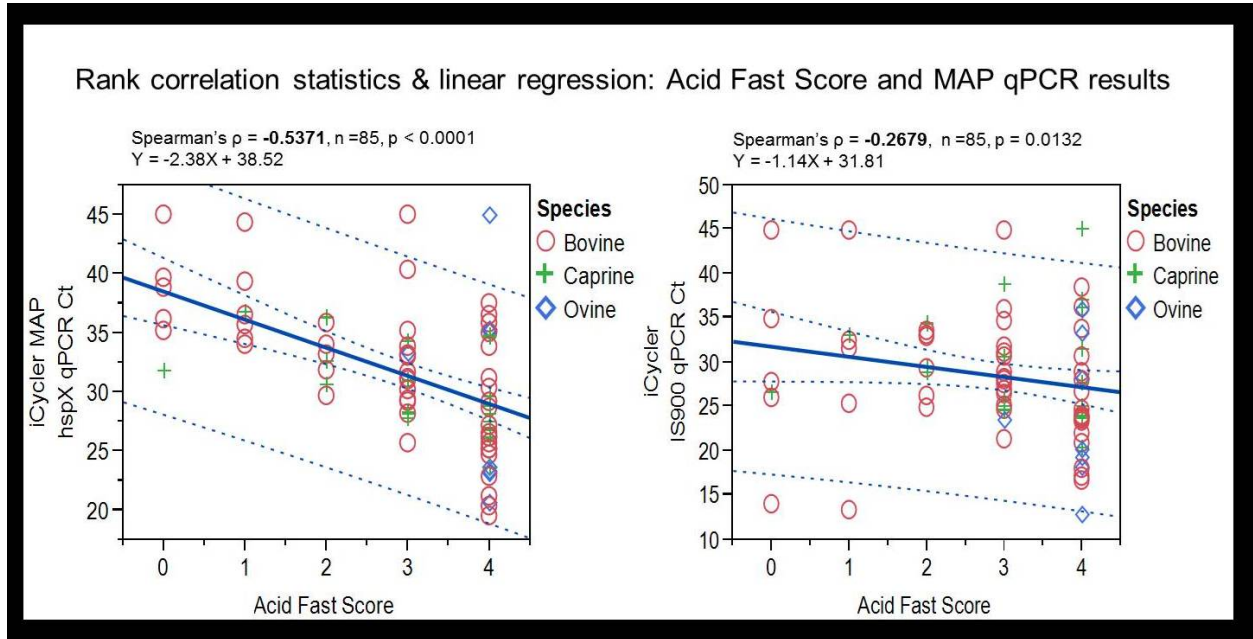


**Figure 3.5** Scatterplot matrices of Acid Fast Bacteria Area Index (AFBAI) & MAP qPCR Cycle threshold (Ct) results.

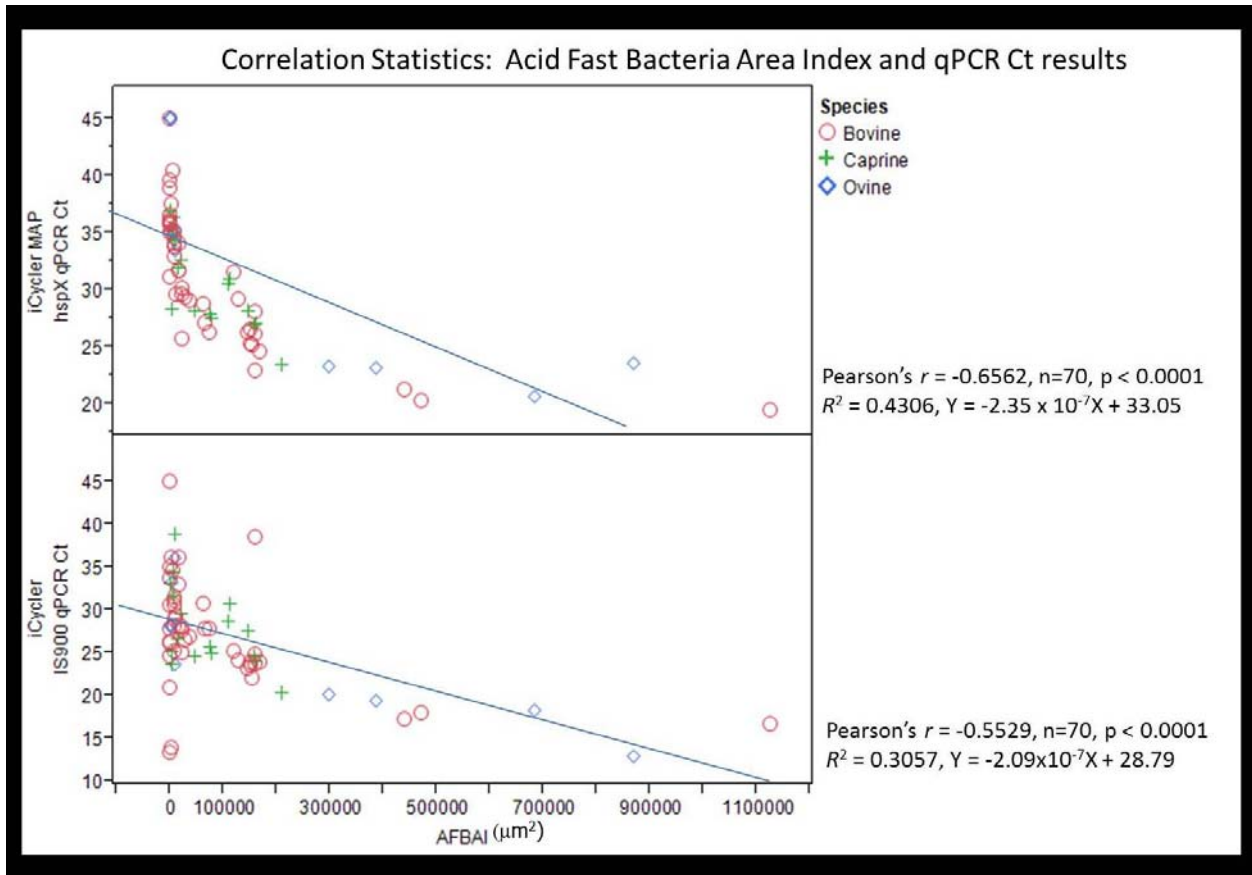
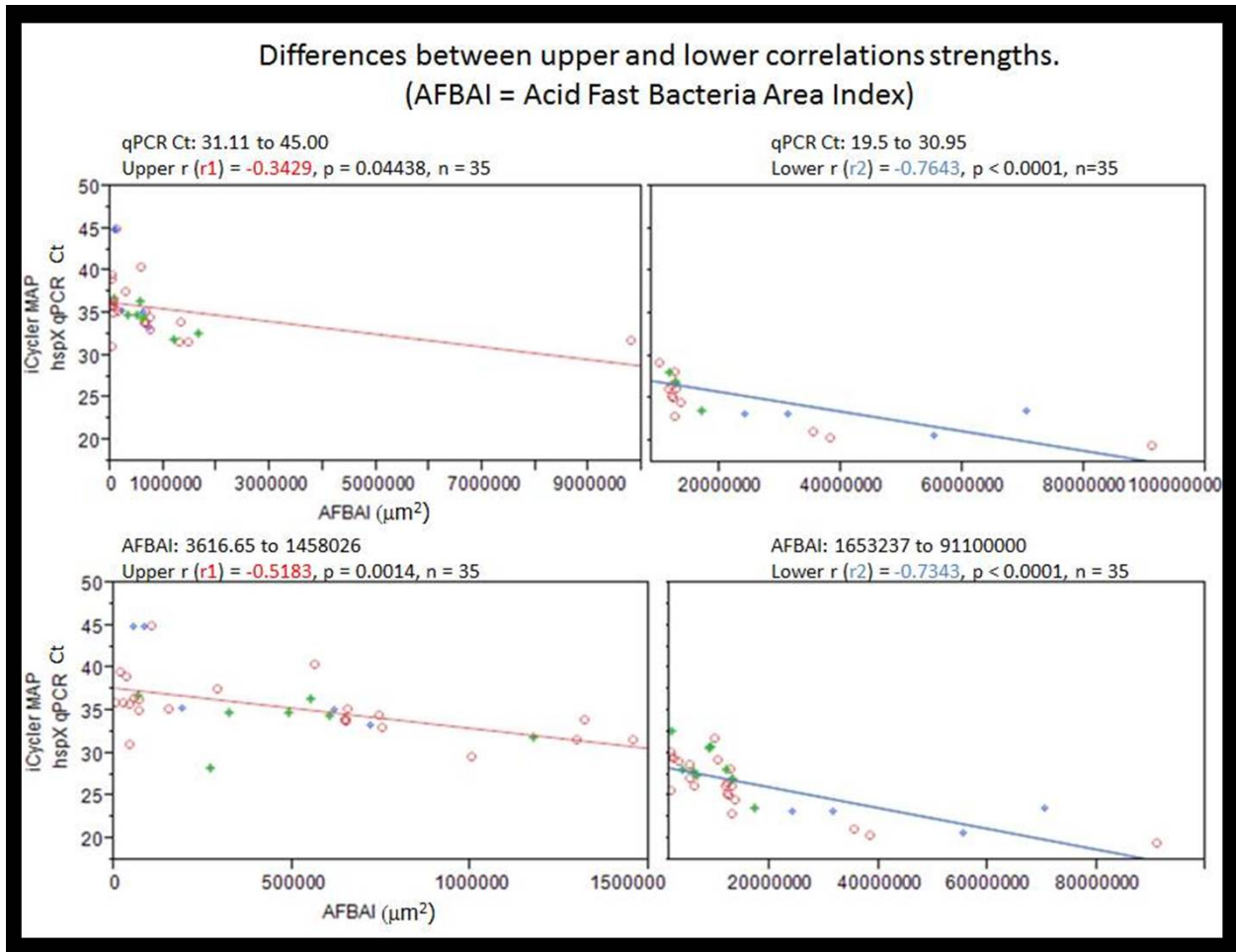


**Figure 3.6:** Scatterplot matrices showing differences between correlation strengths by iCycler MAP *hspX* qPCR Ct results and acid fast bacteria area index (AFBAI) results.



## Tables

**Table 3.1:** BioRad iCycler MAP *hspX* PCR results by acid-fast score for 85 FFPE scrolls from seventy Johne's disease cases, plus thirty-four from eight uninfected animals and 6 non-paratuberculosis mycobacterial infected tissues. FFPE blocks contained either small intestine or mesenteric lymph node (or both) with granulomatous inflammation.

Acid-fast score (number of cases):	Number (%) qPCR-positive	Mean Ct	Number (%) qPCR-negative
4 (40)	38 (95%)	28.83 ± 6.13	2 (5.0%)
3 (21)	19 (90.5%)	31.88 ± 4.43	2 (9.5%)
2 (11)	11 (100%)	32.41 ± 2.29	0 (0.0%)
1 (7)	5 (71.4%)	37.32 ± 3.53	2 (28.6%)
0 (6)	3 (50.0%)	37.80 ± 4.48	3 (50%)
Uninfected :	0 (0%)	>38	34 (100%)
Total cases (n=85)	76 (89.4%)	31.38 ± 5.83	9 (10.6%)
Cases with visible AFB (scores 1-4; n=79)	79 (92.9%)	Mean ± SD	6 (7.1%)

**Table 3.2:** Average acid fast score (AFS), average iCycler MAP *hspX* qPCR cycle threshold (Ct) results and correlation statistics by species

Species	# of animals	# of FFPE blocks	Mean AFS +/- stdev	Mean iCycler MAP <i>hspX</i> qPCR Ct +/- stdev.	% Positive	# Neg / # FN	AFBAI & qPCR Ct correlations
Bovine	45	55	2.6215 +/- 1.3105	32.9987 +/- 5.6954	94%	4 Neg / 3 FN	$r = 0.6511, n = 44, P < 0.0001$
Caprine	17	21	2.8837 +/- 1.1507	31.8998 +/- 3.5947	100%	0 Neg / 0 FN	$r = -0.7954, n = 17, p < 0.0001$
Ovine	8	9	3.8889 +/- 0.3333	31.6411 +/- 9.4171	78%	0 Neg / 2 FN	$r = -0.7957, n = 9, p = 0.0103$

AFS = Acid Fast Score, stdev = standard deviation, Neg = negative by iCycler MAP *hspX* & IS900 qPCR, FN = negative by iCycler MAP *hspX* but positive by IS900 qPCR, AFBAI = Acid Fast Bacteria Area Index

## References:

- 1 Alexander DC, Turenne CY, Behr MA: Insertion and deletion events that define the pathogen *Mycobacterium avium* subsp. *paratuberculosis*. *J Bacteriol* **191**: 1018-1025, 2009
- 2 Buergelt CD, Hall C, McEntee K, Duncan JR: Pathological evaluation of paratuberculosis in naturally infected cattle. *Vet Pathol* **15**: 196-207, 1978
- 3 Carrigan MJ, Seaman JT: The pathology of Johne's disease in sheep. *Aust Vet J* **67**: 47-50, 1990
- 4 Clarke CJ, Little D: The pathology of ovine paratuberculosis: gross and histological changes in the intestine and other tissues. *J Comp Pathol* **114**: 419-437, 1996
- 5 Collins DM, Gabric DM, de Lisle GW: Identification of two groups of *Mycobacterium paratuberculosis* strains by restriction endonuclease analysis and DNA hybridization. *J Clin Microbiol* **28**: 1591-1596, 1990
- 6 Collins MT, Gardner IA, Garry FB, Roussel AJ, Wells SJ: Consensus recommendations on diagnostic testing for the detection of paratuberculosis in cattle in the United States. *J Am Vet Med Assoc* **229**: 1912-1919, 2006
- 7 Corpa JM, Garrido J, Garcia Marin JF, Perez V: Classification of lesions observed in natural cases of paratuberculosis in goats. *J Comp Pathol* **122**: 255-265, 2000
- 8 Dedhia P, Tarale S, Dhongde G, Khadapkar R, Das B: Evaluation of DNA extraction methods and real time PCR optimization on formalin-fixed paraffin-embedded tissues. *Asian Pac J Cancer Prev* **8**: 55-59, 2007
- 9 Ellingson JL, Bolin CA, Stabel JR: Identification of a gene unique to *Mycobacterium avium* subspecies *paratuberculosis* and application to diagnosis of paratuberculosis. *Mol Cell Probes* **12**: 133-142, 1998

- 10 Ellingson JL, Stabel JR, Bishai WR, Frothingham R, Miller JM: Evaluation of the accuracy and reproducibility of a practical PCR panel assay for rapid detection and differentiation of *Mycobacterium avium* subspecies. *Mol Cell Probes* **14**: 153-161, 2000
- 11 Fukunaga H, Murakami T, Gondo T, Sugi K, Ishihara T: Sensitivity of acid-fast staining for *Mycobacterium tuberculosis* in formalin-fixed tissue. *Am J Respir Crit Care Med* **166**: 994-997, 2002
- 12 Gonzalez J, Geijo MV, Garcia-Pariente C, Verna A, Corpa JM, Reyes LE, Ferreras MC, Juste RA, Garcia Marin JF, Perez V: Histopathological classification of lesions associated with natural paratuberculosis infection in cattle. *J Comp Pathol* **133**: 184-196, 2005
- 13 Graham AR, Sobonya RE, Bronnimann DA, Galgiani JN: Quantitative pathology of coccidioidomycosis in acquired immunodeficiency syndrome. *Hum Pathol* **19**: 800-806, 1988
- 14 Grinberg LM, Abramova FA, Yampolskaya OV, Walker DH, Smith JH: Quantitative pathology of inhalational anthrax I: quantitative microscopic findings. *Mod Pathol* **14**: 482-495, 2001
- 15 Harris NB, Barletta RG: *Mycobacterium avium* subsp. paratuberculosis in Veterinary Medicine. *Clin Microbiol Rev* **14**: 489-512, 2001
- 16 Irengue LM, Walravens K, Govaerts M, Godfroid J, Rosseels V, Huygen K, Gala JL: Development and validation of a triplex real-time PCR for rapid detection and specific identification of *M. avium* sub sp. paratuberculosis in faecal samples. *Vet Microbiol* **136**: 166-172, 2009

- 17 Janagama HK, Jeong K, Kapur V, Coussens P, Sreevatsan S: Cytokine responses of bovine macrophages to diverse clinical *Mycobacterium avium* subspecies paratuberculosis strains. *BMC Microbiol* **6**: 10, 2006
- 18 Lambeth C, Reddacliff LA, Windsor P, Abbott KA, McGregor H, Whittington RJ: Intrauterine and transmammary transmission of *Mycobacterium avium* subsp paratuberculosis in sheep. *Aust Vet J* **82**: 504-508, 2004
- 19 Lambrecht RS, Carriere JF, Collins MT: A model for analyzing growth kinetics of a slowly growing *Mycobacterium* sp. *Appl Environ Microbiol* **54**: 910-916, 1988
- 20 Manning EJ, Collins MT: *Mycobacterium avium* subsp. paratuberculosis: pathogen, pathogenesis and diagnosis. *Rev Sci Tech* **20**: 133-150, 2001
- 21 Motiwala AS, Janagama HK, Paustian ML, Zhu X, Bannantine JP, Kapur V, Sreevatsan S: Comparative transcriptional analysis of human macrophages exposed to animal and human isolates of *Mycobacterium avium* subspecies paratuberculosis with diverse genotypes. *Infect Immun* **74**: 6046-6056, 2006
- 22 Motiwala AS, Strother M, Amonsin A, Byrum B, Naser SA, Stabel JR, Shulaw WP, Bannantine JP, Kapur V, Sreevatsan S: Molecular epidemiology of *Mycobacterium avium* subsp. paratuberculosis: evidence for limited strain diversity, strain sharing, and identification of unique targets for diagnosis. *J Clin Microbiol* **41**: 2015-2026, 2003
- 23 Mygind T, Birkelund S, Falk E, Christiansen G: Evaluation of real-time quantitative PCR for identification and quantification of *Chlamydia pneumoniae* by comparison with immunohistochemistry. *J Microbiol Methods* **46**: 241-251, 2001

- 24 Perez V, Garcia Marin JF, Badiola JJ: Description and classification of different types of lesion associated with natural paratuberculosis infection in sheep. *J Comp Pathol* **114**: 107-122, 1996
- 25 Plante Y, Remenda BW, Chelack BJ, Haines DM: Detection of *Mycobacterium paratuberculosis* in formalin-fixed paraffin-embedded tissues by the polymerase chain reaction. *Can J Vet Res* **60**: 115-120, 1996
- 26 Ravva SV, Stanker LH: Real-time quantitative PCR detection of *Mycobacterium avium* subsp. *paratuberculosis* and differentiation from other mycobacteria using SYBR Green and TaqMan assays. *J Microbiol Methods* **63**: 305-317, 2005
- 27 Rowe MT, Grant IR: *Mycobacterium avium* ssp. *paratuberculosis* and its potential survival tactics. *Lett Appl Microbiol* **42**: 305-311, 2006
- 28 Schonenbrucher H, Abdulmawjood A, Failing K, Bulte M: New triplex real-time PCR assay for detection of *Mycobacterium avium* subsp. *paratuberculosis* in bovine feces. *Appl Environ Microbiol* **74**: 2751-2758, 2008
- 29 Shi SR, Cote RJ, Wu L, Liu C, Datar R, Shi Y, Liu D, Lim H, Taylor CR: DNA extraction from archival formalin-fixed, paraffin-embedded tissue sections based on the antigen retrieval principle: heating under the influence of pH. *J Histochem Cytochem* **50**: 1005-1011, 2002
- 30 Sigurdardottir OG, Press CM, Saxegaard F, Evensen O: Bacterial isolation, immunological response, and histopathological lesions during the early subclinical phase of experimental infection of goat kids with *Mycobacterium avium* subsp. *paratuberculosis*. *Vet Pathol* **36**: 542-550, 1999

- 31 Stehman SM: Paratuberculosis in small ruminants, deer, and South American camelids. *Vet Clin North Am Food Anim Pract* **12**: 441-455, 1996
- 32 Stevenson K, Hughes VM, de Juan L, Inglis NF, Wright F, Sharp JM: Molecular characterization of pigmented and nonpigmented isolates of *Mycobacterium avium* subsp. paratuberculosis. *J Clin Microbiol* **40**: 1798-1804, 2002
- 33 Storset AK, Hasvold HJ, Valheim M, Brun-Hansen H, Berntsen G, Whist SK, Djonne B, Press CM, Holstad G, Larsen HJ: Subclinical paratuberculosis in goats following experimental infection. An immunological and microbiological study. *Vet Immunol Immunopathol* **80**: 271-287, 2001
- 34 Taddei R, Barbieri I, Pacciarini ML, Fallacara F, Belletti GL, Arrigoni N: *Mycobacterium porcium* strains isolated from bovine bulk milk: implications for *Mycobacterium avium* subsp. paratuberculosis detection by PCR and culture. *Vet Microbiol* **130**: 338-347, 2008
- 35 Thilagarajah R, Witherow RO, Walker MM: Quantitative histopathology can aid diagnosis in painful bladder syndrome. *J Clin Pathol* **51**: 211-214, 1998
- 36 Valentin-Weigand P, Goethe R: Pathogenesis of *Mycobacterium avium* subspecies paratuberculosis infections in ruminants: still more questions than answers. *Microbes Infect* **1**: 1121-1127, 1999
- 37 Vary PH, Andersen PR, Green E, Hermon-Taylor J, McFadden JJ: Use of highly specific DNA probes and the polymerase chain reaction to detect *Mycobacterium paratuberculosis* in Johne's disease. *J Clin Microbiol* **28**: 933-937, 1990
- 38 Verna AE, Garcia-Pariente C, Munoz M, Moreno O, Garcia-Marin JF, Romano MI, Paolicchi F, Perez V: Variation in the immuno-pathological responses of lambs after

- experimental infection with different strains of *Mycobacterium avium* subsp. paratuberculosis. *Zoonoses Public Health* **54**: 243-252, 2007
- 39 Whittington RJ, Reddacliff L, Marsh I, Saunders V: Detection of *Mycobacterium avium* subsp paratuberculosis in formalin-fixed paraffin-embedded intestinal tissue by IS900 polymerase chain reaction. *Aust Vet J* **77**: 392-397, 1999
- 40 Whittington RJ, Windsor PA: In utero infection of cattle with *Mycobacterium avium* subsp. paratuberculosis: a critical review and meta-analysis. *Vet J* **179**: 60-69, 2009
- 41 Zsikla V, Baumann M, Cathomas G: Effect of buffered formalin on amplification of DNA from paraffin wax embedded small biopsies using real-time PCR. *J Clin Pathol* **57**: 654-656, 2004

## CONCLUSION

### Summary

This research evaluated the performance of a commercial paratuberculosis *hspX* based qPCR assay applied to formalin-fixed, paraffin-embedded (FFPE) tissues using a simple freeze/boil DNA extraction technique. This research compared the results of the paratuberculosis qPCR assay to quantitative histopathology using two methods, an acid fast bacteria score and an acid fast bacteria area index.

### Conclusion

Quantitative PCR assays for paratuberculosis provide a new valuable tool for detecting MAP DNA from FFPE tissues. MAP DNA can be consistently extracted from FFPE tissues by a simple freeze/boil technique and used in commercial qPCR assays to detect MAP DNA. The sensitivity of the commercial paratuberculosis qPCR assays in detecting MAP DNA was greater than 92%. The specificity of the MAP *hspX* based commercial paratuberculosis qPCR assay was 100%. The tested sensitivity of the IS900 based commercial paratuberculosis qPCR assay was 100%.

The qPCR results from the *hspX* assay had the strongest correlation with quantitative histopathology compared to the IS900 based paratuberculosis assay. This is expected because the number of IS900 genes varies from 12 to 20 copies in the MAP genome whereas there is only one *hspX* gene in the MAP genome. Finally, this research showed the correlation between quantitative histopathology and qPCR was strongest using the described acid fast bacteria area index (AFBAI) and the correlation strength between the qPCR and quantitative histopathology increased as the number of bacteria in the FFPE tissues increased (higher AFBAI values & lower qPCR Ct values).

In conclusion, the freeze/boil DNA extraction technique produces a reliable and consistent sample for test by the paratuberculosis qPCR assays and do not seem to be affected by time spent in embedded in paraffin. The sensitivity of the assay is high and relative to the acid fast histopathology. Additionally, the qPCR results (MAP hspX and IS900) both correlate well with the quantity of acid fast bacteria in the FFPE tissues. With this information, this test provides a new valuable tool that can be applied in diagnostic pathology and clinical microbiology. In a diagnostic capacity these qPCR assays provides strong species specific confirmation of paratuberculosis or Johne's disease. This test provides support for the diagnosis of paratuberculosis or Johne's disease when scant or no acid fast bacteria are visible. In a clinical research capacity, these commercial paratuberculosis qPCR assay could be used to measure or detect changes or differences within populations (e.g. treatment response, geographic, sex, breed, species, ages, etc.). Finally, this new reliable and consistent paratuberculosis qPCR assay greatly expands and strengthens the tools available for studying Johne's disease or paratuberculosis.